Evaluation of Cytotoxicity and Genotoxicity of CuO Nanostructures - Potential Anticancer Therapeutics

By

HUDA SHAKIL

97-FBAS/MSBT/S14

Department of Bioinformatics and Biotechnology

Faculty of Basic and Applied Sciences

International Islamic University, Islamabad

2016

International Islamic University
CENTRAL LIBRARY
Islamabad

Accession No. TH 17335

MS
616.994
HUE

Cancer
Infection- Treatment.
Anticance treatment.

Evaluation of Cytotoxicity and Genotoxicity of CuO Nanostructures - Potential Anticancer Therapeutics

By

HUDA SHAKIL 97-FBAS/MSBT/S14

Supervisor: Dr. Asma Gul

Co-supervisor: Dr. Javed Iqbal

Department of Bioinformatics and Biotechnology

Faculty of Basic and Applied Sciences

International Islamic University, Islamabad

2016


بسم الله الرحمن الرحيم

Department of Bioinformatics and Biotechnology

International Islamic University, Islamabad

Dated: 26th February 2016

FINAL APPROVAL

It is certified that we have read the thesis entitled "Evaluation Of Cytotoxicity and Genotoxicity of CuO Nanostructures – Potential Anticancer Therapeutics" and it is our judgment that this project is of sufficient standard to warrant its acceptance by the International Islamic University, Islamabad for the degree of MS Biotechnology.

COMMITTEE

External Examiner
Dr. Rashda Abbasi
Senior Scientific Officer
Institute of Biomedical and Genetic Engineering
G-9/1, Islamabad

Internal Examiner
Dr. Bashir Ahmad
Assistant Professor
Department of Bioinformatics and Biotechnology
International Islamic University, Islamabad

Supervisor
Dr. Asma Gul
Associate Professor
Department of Bioinformatics and Biotechnology
International Islamic University, Islamabad

Co-supervisor

Dr. Javed Iqbal Saggu

Assistant Professor

Department of Physics

International Islamic University, Islamabad

Dr. Javed Iqbal Saggu
Assistant Professor (Physics)
International Islamic University
Islamabad.

Chairperson

Dr. Naveeda Riaz

Associate Professor

Department of Bioinformatics and Biotechnology

International Islamic University, Islamabad

Dean, FBAS

Dr. Muhammad Sher

Professor

Faculty of Basic and Applied Sciences

International Islamic University, Islamabad

A thesis submitted to Department of Bioinformatics and Biotechnology, International Islamic University, Islamabad as a partial fulfillment of the requirements for the degree of MS Biotechnology.

DECLARATION

I hereby declare that the work presented in the following thesis is my own effort except where otherwise acknowledged and that the thesis is my own composition. No part of the thesis has been previously presented for any degree or part thereof.

Date: 26th February 2016

Huda

Huda Shakil

DEDICATION

Dedicated to...

Papa... My moral support throughout life, you taught me to work hard and never give up are the path to triumph!

Mama... My inspiration, it is because of you, your prayers and your encouragement that I have succeeded this far!

☺☺☺

TABLE OF CONTENTS

Acknowledgements

I owe my profound gratitude to **Almighty Allah**, The Creator, The Most Gracious and The Most Merciful. He gave me the courage, health and patience to complete my research work.

I am utterly thankful to my supervisor, **Dr. Asma Gul**, Associate Professor, Department of Bioinformatics and Biotechnology, International Islamic University Islamabad (IIUI), who helped and guided me throughout the project.

I humbly thank my co-supervisor, **Dr. Javed Iqbal**, Assistant Professor, Department of Physics, IIUI, for his support and guidance.

I am highly obliged to my external supervisor, **Dr. Rashda Abbasi**, Senior Scientific Officer (SSO), Institute of Biomedical and Genetic Engineering (IBGE), G-9/1, Islamabad, who not only gave me an opportunity to work in a prestigious institute but also steered, motivated and supported me throughout the research work. I am very grateful.

My humble gratification to **Dr. Abdul Hameed**, Principal Scientific Officer (PSO), and **Dr. Nafees Ahmad**, SSO, IBGE, for your intellectual discussions, constant motivation and technical assistance.

My due respect and regards to **Dr. Naveeda Riaz**, Acting Chairperson, Department of Bioinformatics and Biotechnology, IIUI, and **Dr. M. Ismail**, Director, IBGE, for enabling me to work in an esteemed institute and grant me a chance to polish my skills. Thank you.

I would like to thank **Sadaf Mushtaq**, MS Biotechnology, and **Umar Farooq**, MS Physics, IIUI, for their help and guidance. Last but not the least, I would like to thank my parents, my siblings and friends for their unconditional love and prayers and constant motivation when I was in need of it. Thanks for your constant nudging to keep me go on. I appreciate your enthusiasm, support and care.

May Allah bless you all!

Cheers!! **Huda Shakil**

LIST OF ABBREVIATIONS

%	Percentage
°C	Degree Celsius
Ag	Silver
$AgNO_3$	Silver Nitrate
AO	Acridine Orange
Bax	Bcl-2 asociated X protein
Bcl-2	B-cell lymphoma – 2
bp	Base pair
CH_3COOH	Acetic Acid
Cis	Cisplatin
cm^{-1}	Wavenumber
CO_2	Carbon Dioxide
$CuCl_2$	Copper Chloride
CuO	Copper Oxide
DMSO	Dimethyl Sulfoxide
DNA	Deoxyribonucleic Acid
Dox	Doxorubicin
EDTA	Ethylene Diamine Tetra Acetic Acid
eV	Electron Volt
Fas	Transmembrane Protein

growth. The maintenance of controlled cell growth is regulated by the presence and proper functioning of these genes, if they are not regulated and mutations occur the cells begin to grow irrepressibly (Frederick *et al.*, 2003). During the development of tumors certain hallmarks are acquired by the cancer cells comprising of six biological competencies; continuous and persistent proliferation, overriding growth suppressors, replicative immortality, resistance to cell death, angiogenesis, metastasis (Figure 1.1). This multistep pathogenesis of cancer cells is required for them to be neoplastic, tumorigenic, and to become malignant (Hejmadi, 2010; Hanahan and Weinberg, 2011).

1.2.1.1 Continuous Proliferation

An essential characteristic of a cancer cell is to sustain their proliferation. Normal tissue structure and function is maintained by regulating the production and release of growth promoting factors operating in a paracrine fashion that bind with receptors present on the cell surface containing intracellular tyrosine kinase domains playing a key role in progression of cell cycle. On the contrary cancer cells deregulate these growth signals. They rely on their own intracellular signaling pathways that regulate their progression of cell cycle, having an impact on their cell survival and metabolism. They may yield their own growth signals in autocrine manner or may signal nearby normal cells and obtain growth factors from them (Bhowmick *et al.*, 2004; Cheng *et al.*, 2008). Somatic mutations, increased cell surface receptors, disrupted negative feedback loop all enhance their proliferative ability (Amit *et al.*, 2007; Cabriata and Christofori, 2008; Mosesson *et al.*, 2008; Wertz and Dixit, 2010).

1.2.1.2 Overriding Growth Suppressors

Although cancer cells have an ability to induce growth signals but they must also evade the effects of the negative growth regulators. Tumor suppressor genes have been identified that if function, controls cell proliferation, senescence and apoptosis. For instance genes encoding retinoblastoma associated RB protein and p53 (Sherr and McCormick, 2002; Deshpande *et al.*, 2005; Burkhart and Sage, 2008). Cancer cells deficient of RB and p53 proteins sustain continuous proliferation.

1.2.1.3 Replicative Immortality

Cancer cells require persistent replication in order to produce tumors. Unlike cancer cells, normal cells are able to pass through only a limited number of cell division cycles. They either become senescent or die undergoing a crisis. Cancer cells form cell lines in which the cell surpasses senescence and crisis exhibiting a replicative potential i.e. attain immortality. Telomeres are involved in the immortality of the cancer cells. In mortal cells the telomeres are shortened thus not able to protect the ends of chromosomes that reduces their viability. Telomerase is significantly expressed in immortalized cancer cells, enhancing their chromosome protection by adding repetitive segments to their ends providing resistance to senescence and cell death.

1.2.1.4 Resistance to Cell Death

Cancer cells persistent proliferation and their ability to resist cell death leads to malignant tumors. Apoptosis is triggered in response to the physiological stresses including the signaling imbalance and DNA damage. Apoptosis is considered to be a barrier to the development of cancer. Transduction of extracellular death signals through *Fas* ligand and *Fas* receptor, intracellular signals activating Caspase activity (Caspase 8 and 9) triggers apoptosis, apoptotic bodies are consumed by phagocytosis. Anti-apototic Bcl-2 family bind to and subsequently inhibit pro-apoptotic proteins Bax and Bak and when these two proteins are relieved of the Bcl-2 they release pro-apoptotic signals (cytochrome c). p53, DNA damage sensor and a tumor suppressor induces apoptosis in response to breaks in DNA and chromosomal abnormalities (Junttila and Evan, 2009). The high proliferative rate implicates their apoptosis evasion. The diverse apoptotic signals are to be repressed and surpassed by the cancer cells at multiple levels in order to maintain their cell cycle progression and malignant nature.

1.2.1.5 Angiogenesis

Normal cells as well as tumors require nutrients and oxygen for their growth and need to remove CO_2 and metabolic wastes. Angiogenesis, the process generating neovasculature i.e. development of new blood vessels fulfill their need. Angiogenesis is induced at an early

stage of cancer development. In tumor progression angiogenesis is activated causing the normally dormant vasculature to sprout blood vessels providing nourishment and sustenance to the tumor. Vascular Endothelial Growth Factor-A (VEGF-A) and Thrombospondin-1 (TSP-1) regulate angiogenesis. VEGF-A is a pro-angiogenic factor up regulated by hypoxic environment and oncogene signaling (Carmeliet, 2005; Mac Gabhann and Popel, 2008; Ferrara, 2009). Fibroblast growth factor (FGF) also sustain angiogenesis when it is up regulated unceasingly (Baeriswyl and Christofori, 2009).

1.2.1.6 Metastasis

Cancer cells invade and metastasize to distant parts of the body, changes in their structure and attachment to other cells and the extracellular matrix are typically seen. E-cadherin is lost by the cancer cells which is key factor in cell-cell adhesion (Cavallaro and Christofori, 2004; Berx and van Roy, 2009), whereas its increased expression has been established as an antagonist of metastasis. N-cadherin has been perceived to be up regulated in many cancers. Metastasis follows a cascade of events (Fidler, 2003; Talmadge and Fidler, 2010) involving invasion of the cells in the local tissue, followed by invasion into the blood and lymphatic vessel (intravsatation), escaping of the cancer cells from the vessels into distant tissues (extravestation), finally the formation and growth of small lumps of cancer cells (micrometastases) transformed into colonies.

1.2.2 Apoptosis

Apoptosis is a critical process in cancer progression. Cells that undergo apoptosis endure a well characterized set of changes; cytoplasmic shrinkage, condensation of the nucleus and DNA fragmentation, and eventual lysing of the cells (Kerr *et al.*, 1994). Cancer cells have the ability to avoid apoptosis and continue to propagate. *p53*, 'guardian of the cell', activates specific cell cycle check points and maintains genomic stability. In case of DNA damage it triggers cell cycle arrest and allows the damage to be repaired or proceeds the cell to apoptosis, if the damage cannot be repaired. Bax and Bcl-2 genes are up and down regulators of apoptosis respectively and maintain a cell death balance (Evan and Littlewood, 1998; Maqsood *et al.*, 2013).

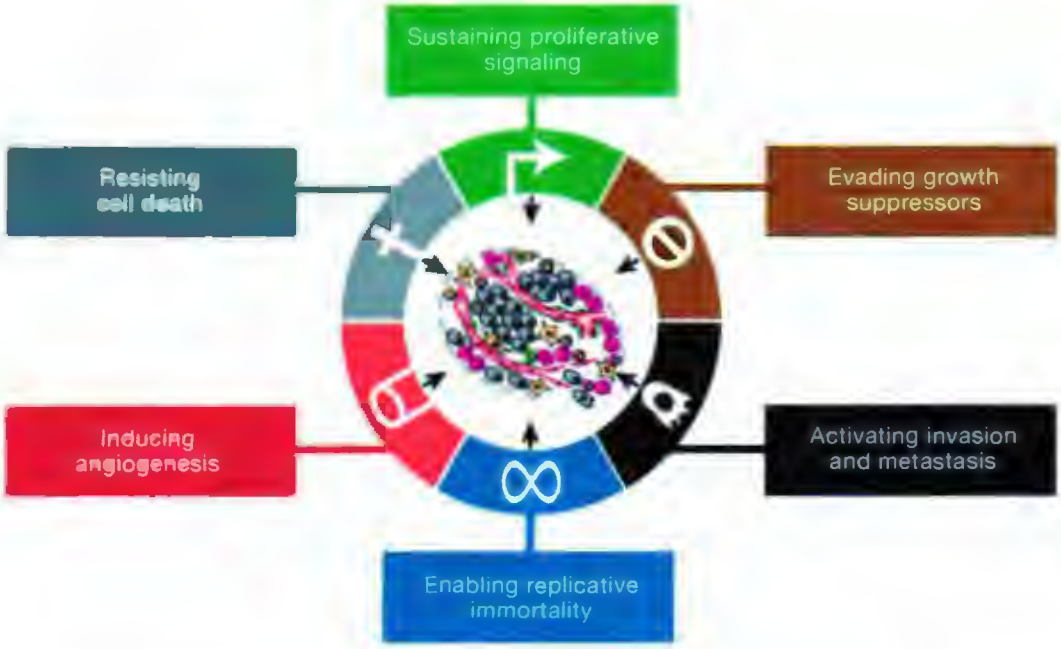

Figure 1.1 Hallmarks of Cancer (Source: Hanahan and Weinberg, 2011)

1.3 Anticancer Treatment

Cancers if treated in time and effectively extends the life of the patient. The anticancer treatments include surgery, chemotherapy and radiotherapy but none of these are ideal modalities of treatment (Jelveh and Chithrani, 2011). The normal cells are also damaged with the chemical and radiation therapies compromising the immune system and the rapidly dividing cells including hair follicles, cells of the bone marrow and the digestive system. The patient acquires other diseases and easily succumbs to a failing health and shortens their life span (Corrie, 2008; Joensuu, 2008; Guo *et al.*, 2015).

1.3.1 Traditional Treatments

1.3.1.1 Surgery:

The type of treatment depends on the type of cancer, its location, and its state of advancement. Surgery is used to remove solid tissue cancers that have not metastasized to other tissues (early stage cancers), and for benign tumors.

1.3.1.2 Radiotherapy:

Radiation kills cancer cells with high energy rays directed directly to the tumor that damages the tumor cells' DNA, compromising DNA replication which induces cell death in the rapidly dividing cells. It also kills normal cells in particular those that divide fast. Surgery and radiation therapy are often used in combination (van Leeuwen *et al.*, 2003).

1.3.1.3 Chemotherapy:

Chemotherapy drugs are toxic chemicals that mostly target the rapid division of cells, some interfere with the synthesis of precursor molecules required for replication of DNA by interfering with the ability of the cell to complete the S phase of cell cycle, while others work by damaging the DNA of the cancerous cells inhibiting the replication process and causing cell death. Spindle inhibitors interrupts the synthesis of microtubules required in cell cycle thus stops replication of cells. As most of the adult cells do not rapidly divide they are less sensitive to these drugs, but cells such as in the lining of the gastro-intestinal

tract, bone marrow cells, hair follicles are sensitive to these drugs as they rapidly divide, resulting in adverse effects of hair loss, low blood cell counts, and gastrointestinal distress (Palumbo *et al.*, 2013).

1.3.1 Innovative Treatments

1.3.2.1 Hormone Therapy:

Although cancer cells lose the normal responses to normal growth hormones, some still require hormones for growth. Hormones effect normal cell growth and hormone therapy includes starving the cancerous cells of the growth hormones, blocking either the activity of the hormone or blocking the synthesis of the hormone altogether (Frederick *et al.*, 2003; Palumbo *et al.*, 2013).

Estrogen is required for the growth of breast cancer cells, drugs called Selective Estrogen Receptor Modulators (SERMs) or anti-estrogens (e.g. Tamoxifen and Raloxifene) block the binding site of the hormone slowing the growth of the cancers. Likewise, testosterone fuels cells of prostate cancer, Selective Androgen Receptor Modulators (SARMs) block the binding of testosterone to the cancer cells, thus preventing prostate cancer.

1.3.2.2 Targeted Chemotherapy:

Advances in chemotherapy have led to development of new chemotherapeutic drugs that target specific active proteins or processes involved in signal transduction pathways, including receptors, growth factors or kinases that are specific to the cancer cells, thus reducing the toxicity to normal cells thus minimizing the side effects (Frederick *et al.*, 2003).

In pancreatic cancer, the oncogene *RAS* is found to be mutated. The RAS protein activates when modified by an addition of a chemical group. Drugs that inhibit the enzyme responsible for the addition of the chemical group to the RAS protein are being considered. Gleevec® prevents growth of cancer cells and cause the cell to undergo apoptosis by

binding to the abnormal proteins which are specific to the cancer cells, hence low toxicity to normal cells.

1.3.2.3 Immunotherapy:

Immune system fails to destroy cancer cells contributing to the development of cancer. Immunotherapy compromises of techniques that use the immune system to attack the cancer cells or treat for the side effects of some cancer treatments. Immuno-stimulators such as interleukin 2 and alpha interferon non-specifically increase immune response against cancer cells.

Chemoimmunotherapy, a technique that ascribes chemotherapeutic drugs to antibodies specific to cancer cells. The antibody delivers the drug to the target without harming normal cells, resulting in reduction of the adverse effects of chemotherapy.

Radioimmunotherapy involves antibodies bound to radioactive atoms targeting the cancer cells with radiation (Vanneman and Dranoff, 2012).

Another immunotherapeutic approach includes, antibodies that inactivate cancer cell specific proteins (growth factors or cancer cell receptors). In breast and ovarian cancer a receptor protein HER2, an antibody Herceptin® binds to the protein and induce cell death by inhibiting the binding of the growth factor to the cancer cell (Frederick *et al.*, 2003).

1.3.2.4 Resistance to Chemotherapy:

With time chemotherapy stops working as the cells become resistant to the therapeutic drugs. In the presence of the drug cancer cells mutate, become resistant to the drug, get the advantage of survival and divide and replicate in the presence of the drug, resulting in a tumor resistant to the therapeutic compounds. Combinations of drugs are used to overcome the drug resistance but chances of multi-drug resistance always pertain. Cancer cells express a gene called *MDRI* that encodes a membrane protein that prevent drugs from entering the cell, also expels the drugs already present in the cell. Some cancer cells make large amounts of this protein and keeps the chemotherapeutic drugs out of them (Frederick *et al.*, 2003; Palumbo *et al.*, 2013).

Angiogenesis can be a target for cancer therapy, naturally occurring proteins, angiostatin and endostatin, prevent angiogenesis, as they do not target directly the cancer cells, therefore there is a less chance of drug resistance.

1.3.3 Nanotechnology

Nanotechnology is an emerging branch of science which is a combination of other fields of sciences including physics, chemistry, and biology. It has come up with the concept of nanostructures' synthesis from respective metals, their oxides and alloys. To date, many different nanostructures such as nanoparticles, nanowires etc. have been synthesized for various applications (Ferrari, 2005).

1.3.3.1 Classification of Nanomaterials

Nanomaterials have been prepared over a wide range of sizes, shapes and forms. Nanoarchitectonics has been proposed as a system to arrange structural units at a nanoscale in a pre-designated alignment (Katsuhiko *et al.*, 2011). Unlike bulk material, nanostructures have finite forms due to their low dimension. Therefore, restricted number of nanostructure classes exist; Zero Dimensional (0D), One Dimensional (1D), 2 Dimensional (2D), and 3 Dimensional (3D) materials based on the degree of freedom. All kinds of nanostructures known belong to one of these classes (Tiwari *et al.*, 2012; Pokropivny and Skorokhod, 2007).

i. Zero Dimension (0D) Nanomaterials

All three sides of the material are confined at nanoscale. For example, quantum dots, nanoparticles, nanocrystals, and nanospheres.

ii. One Dimension (1D) Nanomaterials

Two out of three sides are confined at nanoscale. Examples include nanorods, nanowires, nanotubes, DNA, nanorings, nanowhiskers, and nanobelts.

iii. Two Dimension (2D) Nanomaterials

One of the three sides is confined at nanoscale. For instance in thinfilms, membranes, quantum-well, interfaces, multi-layers, nanosheets, graphene, self-assemble monolayers, and Langmuir-Blodgett films.

iv. Three Dimension (3D) Nanomaterials

These include bulk materials with nanoscale structural control i.e. nanohybrids, nanocomposites and mesoporous materials (Katushiko *et al.*, 2011; Tiwari *et al.*, 2012).

Nanotechnology represents a new aspect of combinatorial science based on the interfacing concepts of nanomaterials and biological systems. This interface includes their interaction, kinetics and thermodynamic changes between the nanomaterial and their linked biological components including membranes, DNA, RNA, proteins, phospholipids etc. (Bhattacharya *et al.*, 2012).

Researchers have gained interest in nanotechnology due to the unique properties of nanomaterials including increased conductivity, toughness, hardness and strength of metals and their alloys, luminescent efficiency of semiconductors, and formability of ceramics.

Nanomaterials have found many applications in different fields like electronics, medicine, pharmaceuticals, therapeutics, textile industries, and in food packaging with the advancement in the field of nanotechnology (Duncan, 2011; Cohen-Karni *et al.* 2012; Bhattacharya *et al.* 2012). Specifically metal nanomaterials, ranging from size 1–100 nm possess unique properties like physicochemical, electrical, optical, and most important biological properties and thus have been manufactured at a large scale for different industrial and household applications (Chang *et al.*, 2012; Ingle *et al.*, 2014).

1.3.4 Nanomedicine

The application of nanotechnology termed as Nanomedicine is a concept that involves the use of engineered materials at a nanoscale to develop novel diagnostic and therapeutic modalities (Jelveh and Chithrani, 2011) that are highly prospective in cancer management

in particular, and in other healthcare areas (Freitas, 2005; Farokhzad and Langer, 2006; Liu *et al.*, 2007; Bhattacharya *et al.*, 2012).

A wide variety of therapeutics based on nanotechnology have been developed for various diseases that have high rates of mortality such as cancer, cardiovascular diseases, diabetes, rheumatoid arthritis and asthma (Brannon-Peppas and Blanchette, 2004; Kawasaki and Player, 2005)

Nanostructures are used as molecular probes, they can be used to inspect cellular machinery without much interference due to their size. The cells of a living organism have a size of approximately 10μm and the intercellular components such as the organelles, DNA, RNA and some proteins have sizes much smaller having a dimension of just 5nm which are comparable to the size of nano-materials synthesized by humans (Taton, 2002; Paddock, 2012).

Nanostructures also have photoluminescence ability and have capacity for drug loading and can thus play an important part in targeted delivery of drugs and can be used as imaging agents as well (Abhijeet *et al.*, 2014).

As compared to traditional cancer medicines nanomaterials are much more specific (Frank *et al.*, 2010) due to their targeted localization in cancerous area and vigorous cellular uptake (Mark *et al.*, 2008; Zhang, 2012). Nowadays magnetic and super-paramagnetic nanostructures are being synthesized for specific target site to achieve highly efficient carcinogenic cell destruction (Manuel *et al.*, 2013; Alireza *et al.*, 2014).

1.3.5 Copper Oxide Nanoparticles (CuO)

Copper oxide or cupric oxide has a narrow band gap of 1.2 eV (Tran and Nguyen, 2014). CuO although the simplest member of copper compounds having a monoclinic structure, displays physical features such as high temperature superconductivity, spin dynamics, and photovoltaic and photoconductive properties due to its narrow band gap. CuO nanostructures can also improve fluid viscosity and enhance thermal conductivity making them an energy saving material, they can be used in industrial catalysis and lubricants as

they can reduce friction, and in metallic coatings as they can mend worn out surfaces. It has also been used as ceramic resistors, gas sensors, magnetic storage media, semiconductors, near-infrared tilters. CuO nanostructures have unusually high surface areas and unusual crystal morphologies which gives them specific antimicrobial activity (Chang *et al.*, 2012; US Research Nanomaterials, Inc.; AzoNano, 2013).

Copper is a trace element found in all living organisms and is important for their growth and development. It is required for the function of several enzymes and proteins that are involved in metabolism, respiration, DNA synthesis, superoxide dismutase, ascorbate oxidase, tyrosinase, and cytochrome oxidase. As copper is involved in oxidation reduction reactions, they directly interact with molecular oxygen and produces free radicals. Therefore mechanisms to control copper levels are tightly controlled to remove any toxic effects (Tisato *et al.*, 2010). Copper and its complexes have found variety of uses such as in disinfection of water, algaecide, fungicide, and as antifouling agent (Perelshtein *et al.*, 2009).

Copper oxide nanostructures are shown to have antibacterial and antiviral activities, they have been used in wound dressings, face masks and socks (Borkow and Gabbay, 2004; Gabbay *et al.* 2006; Borkow *et al.* 2009; Borkow *et al.* 2010; Bondarenko *et al.*, 2013) Copper oxide nanostructures are known to be cytotoxic to hepatocellular carcinoma HepG2 cell line mediated through ROS production causing oxidative stress (Maqsood *et al.*, 2013; Vinardell and Mitjans, 2015).

CuO showed cytotoxicity in cell type non-specific manner. Release of Cu^{2+} ions from CuO has also been reported as the most likely cause of toxicity in cancer cells (Chusuei *et al.*, 2013).

1.3.5.1 Synthesis

Copper based nanostructures can be synthesized by numerous techniques involving the chemical, physical and biological techniques (Ingle *et al.*, 2014). Studies have reported biosynthesis of copper oxide nanoparticles from plant extracts of *Ficus religiosa* or *Acalypha indica* (Sankar *et al.*, 2014; Vinardell and Mitjans, 2015). Chemical methods

such as thermal evaporation, sono-chemical, sol-gel, electrochemical and hydrothermal methods have been developed for the production of Copper oxide nanostructures (Dar *et al.*, 2009; Toboonsung and Singjai, 2011). Chemical methods for preparation of Copper oxide nanostructures offer advantages such as high uniformity of size and shape of the nanomaterial prepared, lower amounts of waste of raw materials, large scale production with a low investment of capital, and it allows use of low cost and high throughput equipment (Tan and Nguyen, 2014).

1.3.6 Metal Ion Doping

Nanomaterials are doped with ions of foreign elements to impart desired electronic, magnetic and optical properties in them. Recently, modification and addition of impurities in nanomaterials has been shown to have an impact on the growth of several functional nanostructures and provides an approach to adjust the crystallographic phase, size, morphology and electronic configuration of nanomaterials (Chen and Wang, 2013).

The cancer cell specificity of CuO nanoparticles is expected to be improved by doping, making them less toxic to the normal cells and more cytotoxic to the cancer cells at smaller size range and lower doses.

1.3.7 Ag Nanostructures

Since ancient times, bulk silver and silver compounds have been used to prevent and fight of infections. At present time silver nanostructures are commercialized in products such as detergents, nutritional supplements, cosmetics, and surface coatings in water purification systems (Marambio-Jones and Hoek, 2010; Bondarenko *et al.*, 2013). Silver nanostructures (Ag NPs) are known to be antibacterial, antifungal, antihelminthic and antiviral, they also facilitate healing of wounds. They have been found to be cytotoxic to cancer cells (Opinath *et al*, 2008; Gopinath *et al.*, 2010; Selvi and Sivakumar, 2014).

Ag nanostructures induce cytotoxicity, are able to penetrate biological barriers and induce immune responses. ROS generation and the ability to dissociate into ions depends on their

size. Smaller the size of the particles more readily their uptake into the cell and more is their cytotoxic potential (Liu *et al.*, 2010).

Ag NPs induce damage to endothelial cells changing their morphology, increase their permeability, and induce cytokine release thus inducing immunological responses. Ag NPs cause leakage of cathepsins from lysosomes, produce higher amounts of hydrogen peroxide, and superoxides in mitochondrial membranes, a determinant of their cytotoxicity (Zhang *et al.*, 2014).

Silver nanostructures were found to selectively inhibit cancer cell growth as compared to normal cells (Soenen *et al.*, 2013). Introduction of Ag with other nanostructures has been reported to enhance their anticancer activity (Arooj *et al.*, 2015).

1.3.8 Mode of Action of CuO

1.3.8.1 Cellular uptake

The cellular uptake and intracellular bioavailability of CuO nanostructures is associated with their cytotoxic potential. Ions enter cells via transporters, while CuO enter cells through endocytosis. The uptake of CuO via endocytosis has been confirmed (Wang *et al.*, 2012). Transmission electron microscopy (TEM) validated CuO entry in human lung carcinoma (A549) cells and organelles including mitochondria, lysosomes and nuclei using endocytosis inhibitors. Endocytosis was the primary pathway involved in cellular uptake, forming endosomes and their transformation into lysosomes (Figure1.2).

1.3.8.2 Escape of Cu^{2+} ions from the surface

Cu^{2+} ions are released from CuO nanostructures in aqueous medium. Release of ions is reported to be a cause of their cytotoxic potential in human bronchial epithelial (BEAS-2B) and human lung carcinoma (A549) cells (Chusuei *et al.*, 2013). The cellular uptake and release of Cu^{2+} ions mediate their cytotoxic effects.

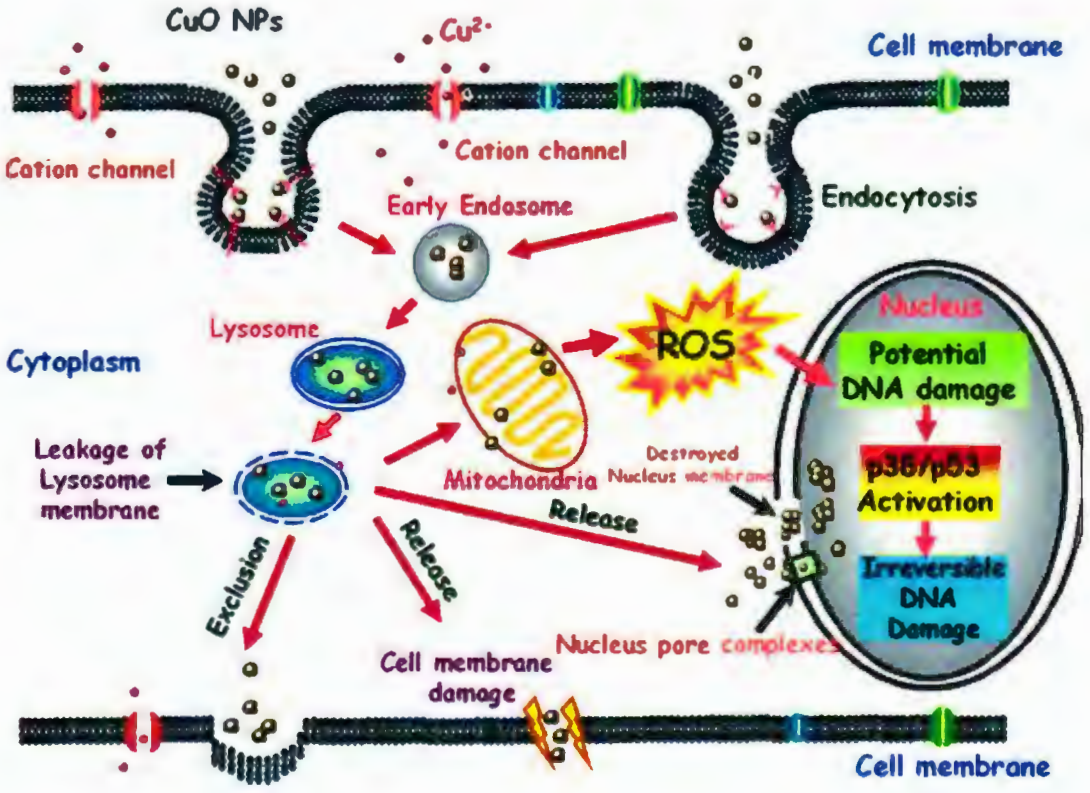

Figure 1.2 Mode of Action of CuO Nanoparticles. CuO enters cell through endocytosis, leads to ROS production, oxidative stress, nuclear damage and genotoxicity (Source: Wang *et al.*, 2012).

FCS	Fetal Calf Serum
FGF	Fibroblast Growth Factor
FTIR	Fourier Transform Infrared Spectroscopy
GPPS	L-Glutamine, Na-pyruvate, Penicillin, and Streptomycin
HepG2	Hepatocellular Carcinoma Cells
IC_{50}	50% Inhibition Concentration
M	Moles
MDA	Malondialdehyde
MDRI	Multidrug Resistant Gene
mg	Milligram
ml	Milliliter
mM	Milli moles
NaCl	Sodium Chloride
NaOH	Sodium Hydroxide
nm	Nanometer
NTC	Untreated Cells
P53	Tumor protein 53
PBS	Phosphate Buffer Saline
PI	Propidium Iodide
RB	Retinoblastoma Protein
RNA	Ribonucleic Acid

ROS	Reactive Oxygen Species
rpm	Revolutions per minute
RPMI – 1640	Roswell Park Memorial Institute 1640
SDS	Sodium Dodecyl Sulfate
SRB	Sulforhodamine B
TBA	Thiobarbituric Acid
TBARS	Thiobarbituric Acid Reactive Substances
TBE	Tris-Borate-EDTA
TCA	Trichloroacetic Acid
TE	Tris-EDTA
TSP-1	Thrombospondin – 1
U	Unit
U937	Histocytic lymphoma cell line
UV	Ultraviolet
V	Volts
VEGF-A	Vascular Endothelial Growth Factor A
XRD	X-ray Diffraction
µg	Microgram
µl	Microliter
µM	Micro moles

LIST OF FIGURES

LIST OF TABLES

Abstract

Cancer is a leading cause of mortality; characterized by cell structural changes, over-expression of proteins and production of new enzymes, growth inhibition of nearby cells, decreased cell adhesion, and invasion of other tissues. Compromised DNA repair mechanisms in cancer cells allows them to evade apoptosis, giving them the ability to proliferate devoid of interruption. A major challenge in cancer therapy is to find agents capable of targeting and penetrating cancer cells, without having adverse effects on normal cells. Nanotechnology provides nanoscale vehicles for targeting cancer cells only eliminating the toxic effects of conventional cancer therapies. In this study, six nanostructures (H-0, H-1, H-3, H-5, H-8, and Ag) were prepared by wet chemical method. Undoped CuO and Ag along with Ag doped CuO nanostructures (1%, 3%, 5% and 8%) were included in this study. These nanostructures were screened for their cytotoxic potential on hepatocellular carcinoma (HepG2) cell line. Cells treated with these nanostructures showed dose dependent decrease in viability. IC_{50} values for the nanostructures revealed inhibitory concentration of doped nanostructures (IC_{50}: 7.89 - 9.77μg/ml) when compared to undoped (IC_{50} CuO: 14.85μg/ml, Ag: 43.66μg/ml) was lowered. Nanostructures were found to induce oxidative stress i.e. lipid peroxidation, DNA degradation, and apoptosis in HepG2 cells. Further *in vitro* analysis of these nanostructures is required to assess their anticancer therapeutic potential and validate these results before proceeding to *in vivo* studies.

INTRODUCTION

INTRODUCTION

1.1 Cancer

Cancer is a disease in which cells divide without control (Selvi and Sivakumar, 2014) and at advance stages are capable of invading other tissues. About 23% of the total deaths in USA are due to cancer, second to that of heart disease. By 2008, only 5–10% cases were accredited to genetic defects, the remaining 90–95% cases were due to other factors such as use of tobacco in 25-30% cases, in 30-35% cases death was due to diet problems and in about 15–20% of the cases infections was the cause of mortality. Other risk factors included stress, radiation, physical activity and environmental pollutants etc. (Anand *et al.*, 2008).

Cancer is becoming a leading cause of death in the Asian countries including Pakistan (Muhammad, 2009). The incidence, prevalence and mortality due to cancer is increasing in Pakistan (GLOBOCAN 2008). Out of every 150,000 new cases 60-80% patients die each year. With high prevalence of hepatitis C and B, hepatocellular cancer is very common and the mortality rate keeps rising in Pakistan (Aasim, 2013). In another report from Shaukat Khanam Memorial Cancer Hospital and Research Center, the most common malignancies in the region are that of breast, lip and oral cavity, and liver and intrahepatic bile duct (Badar and Mahmood, 2015).

Guo *et al.* stated 1.5 million people die of cancer annually in Asia, and the number increases with the passage of time. Changes in living trends and the social environment has been the key factors in the increased incidence of cancer.

1.2 Biological Aspects of Cancer

A normal cell grows, divide, differentiate and perform their functions that allows an organism to thrive. These normal cells when start dividing uncontrollably, start invading other tissues (metastasize), seizing resources from other normal cells results in killing the organism gradually.

Normal cell division is lost, abnormal functions are acquired through mutations that are either inherited or environmentally induced through UV radiation, X-Rays, chemicals, viruses etc. or through internal factors including the Reactive Oxygen species (ROS) production in metabolic processes. Although cells do not become cancerous as a result of one single event of mutation or a single factor. Multiple events are required for cancer cell development that may be lapsed over many years.

As the cancerous cells grow they develop new characteristics i.e. cell structural changes, decreased cell adhesion, over-expression of proteins, production of new enzymes, growth inhibition of nearby cells, allowing them to invade other tissues (Faratian *et al.*, 2010). The DNA damage caused is repaired in normal cells, but in cancerous cells the genes responsible for the DNA repair are themselves compromised and thus mutation rate is increased in these cells. If these cells remain in their original location they are considered benign tumors. If they become invasive and invade other neighboring tissues they are malignant. These malignant cells then travel to other distant parts of the body i.e. metastasize and forms tumors. The type of secondary tumor formed depends on the primary tumor i.e. cell of the tissue initially altered. There are five types of cancers: Carcinomas that are the resultant of transformed epithelial cells that are present on skin and other internal organ's surface; Sarcomas are cancers of bone, fat or connective tissues; Lymphoma cancer of lymphatic system cells derived from the bone marrow; Leukemia is cancer of white blood cells; Myelomas are cancer of cells of the immune system.

1.2.1 Genetic Factors

The genes involved and associated with cancer can be divided into three groups, the proto-oncogenes, the tumor suppressor genes and the DNA repair genes. The proto-oncogenes normally enhance cell division of cells mutations in these genes result in oncogenes that allow uncontrollable cell division. The tumor suppressor genes normally inhibit cell growth and mutations in these genes may result in the loss of their function allowing the cancerous cells to grow and divide. The DNA repair genes are responsible for the repair in genes for their proper functioning, if these genes are compromised, the damage in the genes is not repaired, damages accumulate giving cancer cells advantage over the normal cells in

1.3.8.3 Oxidative Stress

Reactive Oxygen Species (ROS) generation and oxidative damage are important determinants of cytotoxicity induced by CuO. ROS includes hydroxyl radicals (OH^-), superoxides (O_2^-), peroxides (O_2^{2-}) and singlet oxygen ($^1O_2$). ROS are produced normally at low levels in living organisms. Under normal conditions ROS mediated damage is kept under control by antioxidant enzymes including superoxide dismutase, glutathione peroxidase, glutathione reductase and catalase and non-enzymatic antioxidants, ascorbic acid and glutathione α-tocopherol. Excess of ROS cause oxidative stress leading to mitochondrial damage which further increase ROS production, lower mitochondrial function and apoptosis. CuO mediated imbalance in oxidants and antioxidants, causing loss in mitochondrial membrane potential in human lung carcinoma A549 cells has been reported (Ahamed *et al.*, 2015). Intracellular Glutathione reduction and lipid peroxidation in cells exposed to CuO have also been reported (Karlsson *et al.*, 2008; Wang *et al.*, 2012). Reduced catalase and glutathione reductase enzymes and increased levels of glutathione peroxidase activity in response to exposure with CuO nanostructures suggest inhibition of antioxidant mechanisms (Chang *et al.*, 2012; Thit *et al.*, 2015). Cu yields free radicals via Fenton type reaction and impose oxidative stress, cupric ion reuduced to cuprous ion, generating hydroxyl radicals from hydrogen peroxide (Ahamed *et al.*, 2015).

1.3.8.4 Induction of Apoptosis

CuO mediated cell death has been studied and evidence of apoptosis has been reported. Destabilization of mitochondrial integrity and decrease in mitochondrial membrane potential causing cells to undergo apoptosis, when exposed to CuO nanostructures. Bax, bcl-2 and p53 expression analysis also suggest pro-apoptotic capacity of CuO (Maqsood *et al.*, 2013; Thit *et al.*, 2013). CuO induce elevation in sub G1-peak an indication of apoptosis. CuO also caused an increase in Apoptosis Inducing Factor (AIF) translocation into nucleus resulting in release of apoptotic enzymes (Semisch *et al.*, 2014).

1.3.8.5 Genotoxicity

CuO NPs have been theorized to disrupt nuclear membrane allowing the particles to enter the nucleus and interact directly with DNA (Wang *et al.*, 2012). CuO induce DNA strand breaks in HeLa S3 cells mediated by H_2O_2. CuO inhibit poly-ADP-ribosylation. Poly-ADP-ribosylation is a post-translational modification of proteins, where multiple ADP-ribose moieties are attached to histones, transcription factors or DNA repair proteins. This reaction mediates DNA damage signaling and maintains genomic stability (Semisch *et al.*, 2014).

1.4 Objective:

The objective set for this study was to fabricate undoped CuO, and Ag doped CuO nanostructures in varying concentrations (1%, 3%, 5%, and 8%), to characterize the nanostructures synthesized and to investigate their cytotoxic and genotoxic potential on cancer cell line.

MATERIALS AND METHODS

MATERIALS AND METHODS

2.1 Nanomaterial Synthesis

Doped and un-doped Copper Oxide (CuO) nanostructures (Table 2.1) were synthesized using the Co-precipitation method.

CuO nanomaterial was prepared (Tran and Nguyen, 2014) according to the following equations:

$$CuCl_2 + NaOH \longrightarrow Cu(OH)_2 + NaCl$$

$$Cu(OH)_2 \longrightarrow CuO + H_2O$$

2.1.1 Undoped Copper Oxide

Copper Chloride ($CuCl_2$) (AppliChem) was used as a precursor and Sodium Hydroxide (NaOH) (Sigma Chemical Co., USA) was used a reducing agent. $CuCl_2$ was added in a glass beaker containing 100 ml de-ionized water and placed on a heating magnetic stirrer (Corning, PC-420D). The temperature was maintained at 100°C. Glacial Acetic Acid (CH_3COOH) (Scharlau, Scharlab S.L., Spain) was added in the $CuCl_2$ solution with constant and steady stirring for 1 hour. Aqueous NaOH was prepared separately in a beaker and was titrated against $CuCl_2$ solution in a drop wise manner until color change was observed, the clear blue color of $CuCl_2$ changed to an opaque turquoise and then to black, indicating completion of the reaction (Figure 2.1). The solution was then allowed to cool down to room temperature. After 1 hour the sample was washed thrice with de-ionized water, centrifuged at 300 rpm for 5 minutes each time. The sample was dried in drying oven (Carbolite, England) at 300°C, grinded and collected in sample holders.

2.1.2 Silver Doped Copper Oxide

As the concentration of the dopant, silver (Ag), was increased the amount of $CuCl_2$ was decreased. 1%, 3%, 5%, and 8% Ag doped CuO nanostructures were prepared utilizing $AgNO_3$ (Sigma-Aldrich, USA) as a precursor. The respective amounts of $AgNO_3$ was

added to the aqueous solution of $CuCl_2$ prepared in 100ml dH_2O with constant stirring at 100°C. Glacial Acetic Acid (2ml) was added and after 1 hour NaOH was added in a drop wise manner until color change was observed from the clear blue to opaque turquoise and finally to black (Figure 2.2). The solution was stirred for another hour to complete the reaction time. The sample was then washed thrice with de-ionized water. Furthermore, the samples were dried in drying oven, grinded and collected in sample holders.

2.1.3 Silver Nanostructures

Silver Nitrate ($AgNO_3$) was weighed and added in a glass beaker containing 100ml de-ionized water. With constant stirring at 100°C a few drops of NaOH were added so that $AgNO_3$ mixes well in the water. Glacial Acetic Acid (2ml) was added. Next, NaOH was added drop wise until the color of the solution turned dark green and the pH when checked by litmus paper was 10 (Figure 2.3). The reaction time was completed and the solution was allowed to cool down to room temperature. The precipitates that were formed when settled down, the upper aqueous solution was discarded and the sample washed thrice with de-ionized water. The sample was dried in drying oven, grinded and collected in sample holders.

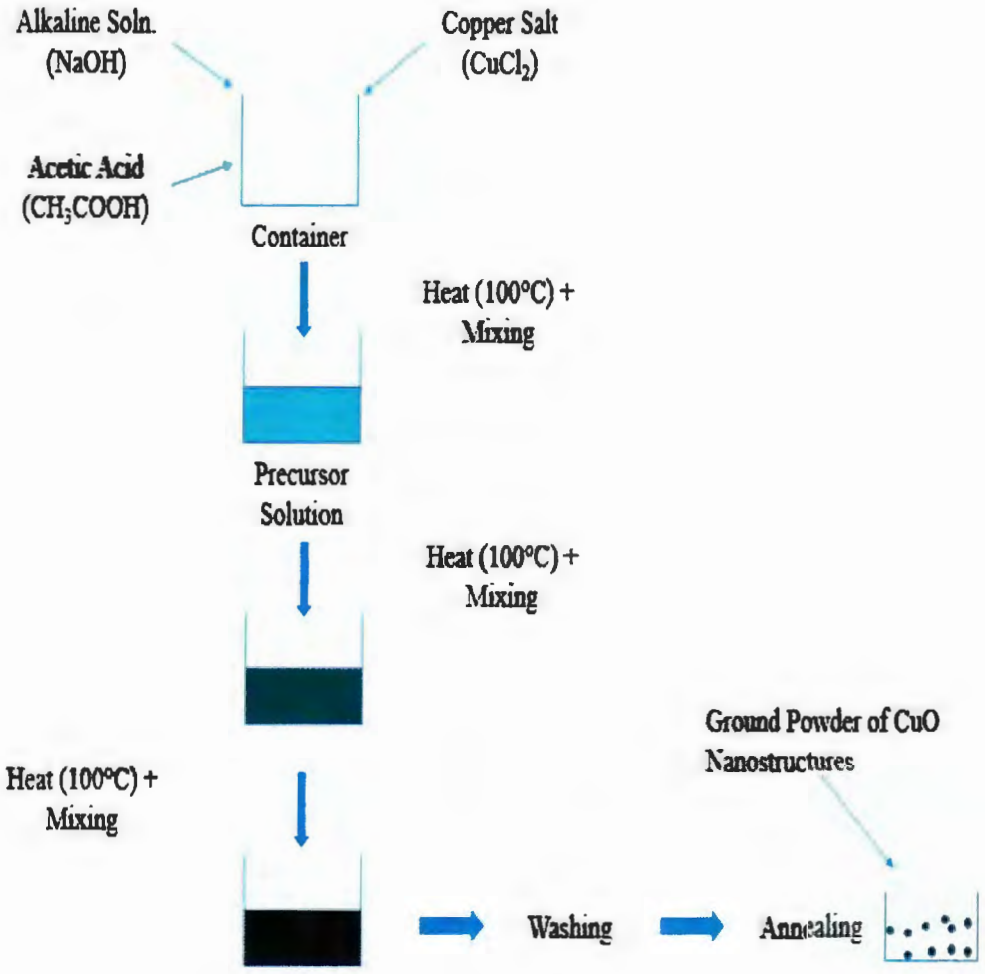

Figure 2.1 Schematic representation of Co-precipitation method for the production of Copper oxide (CuO) nanostructures.

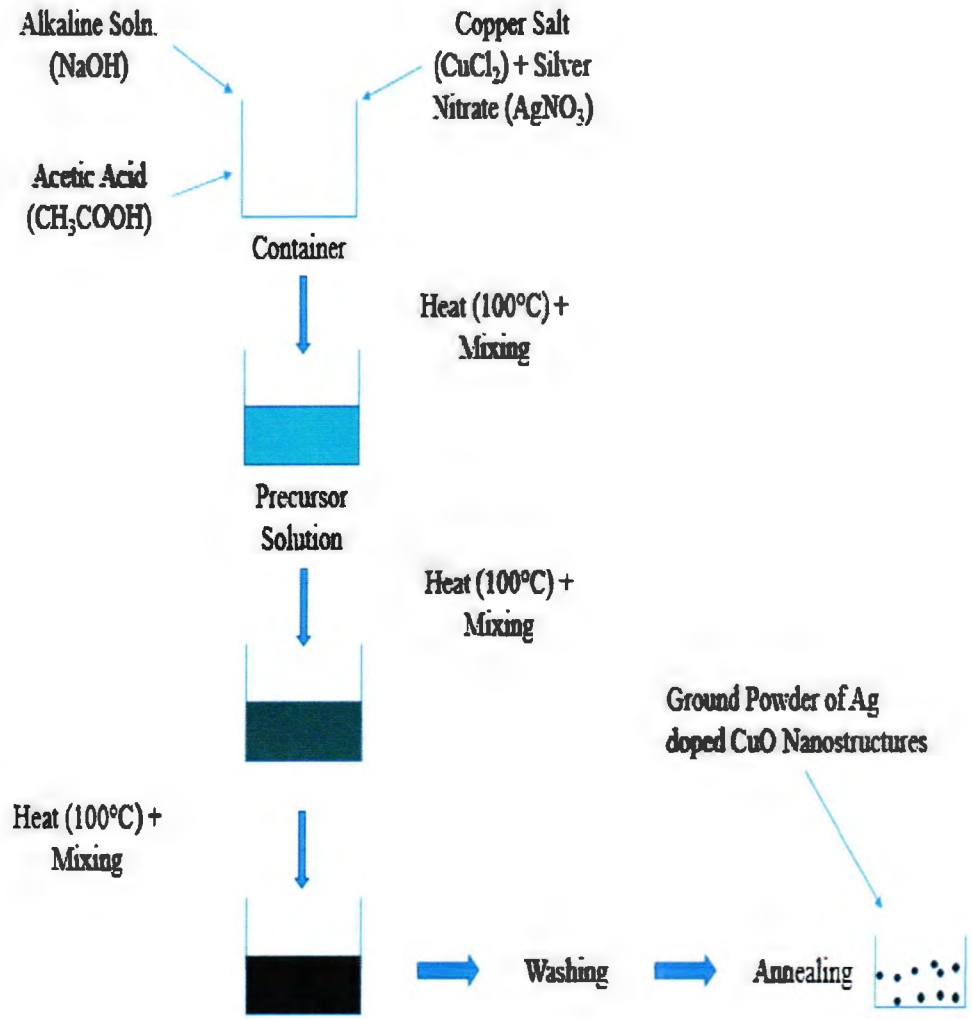

Figure 2.2 Schematic representation of Co-precipitation method for the production of Ag doped Copper oxide (CuO) nanostructures.

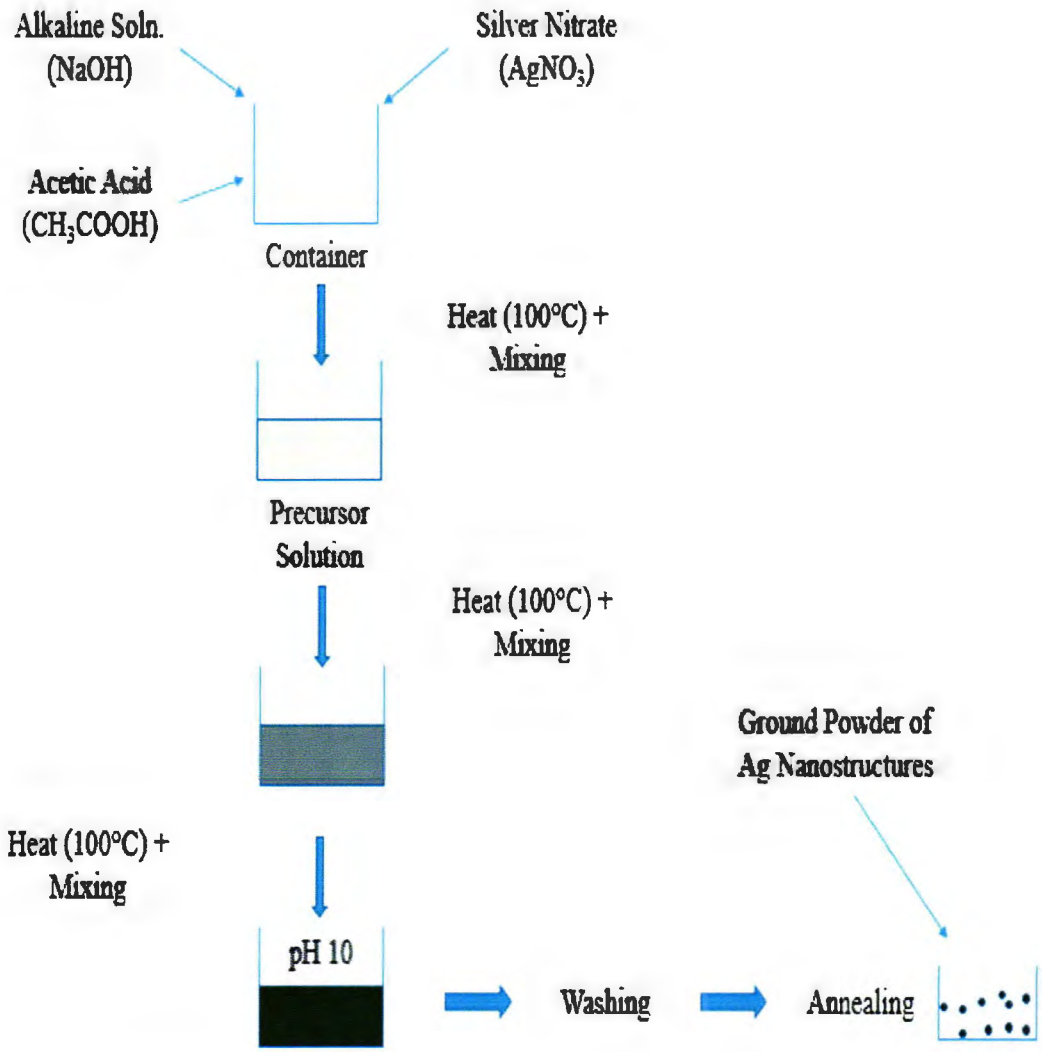

Figure 2.3 Schematic representation of Co-precipitation method for the production of Silver (Ag) nanostructures.

Table 2.1: List of nanostructures prepared.

Sample	Description
H-0	CuO
H-1	1% Ag doped CuO
H-3	3% Ag doped CuO
H-5	5% Ag doped CuO
H-8	8% Ag doped CuO
Ag	Ag

2.2 Characterization of Nanostructures

2.2.1 Scanning Electron Microscopy (SEM)

In SEM, the samples are focused with a beam of electrons, which interact with the atoms of the samples, producing signals which are detected and contains information about the sample. SEM achieves resolution better than 1nm. It was used to study the morphological characteristics of the nanostructures (Goldstein, 1992). The morphology and particle size of the nanostructures were studied by SEM. The nanostructures synthesized were focused with an electron beam of 15kV and the image was produced.

2.2.2 X-ray Diffraction (XRD)

The nanostructures prepared were characterized using X-ray Diffraction (XRD) to understand the crystalline nature and evaluate the average crystallite size of the synthesized structures.

Shimadzo 6000 X-ray spectrophotometer utilizing Cu Kα (λ = 1.54 Å) radiation at 40 kV and 30 mA was used for the XRD analysis of nanostructures. The diffraction patterns were recorded at 2θ = 20 - 70°.

Scherrer's formula was used to estimate the particle size (Ahamed *et al.*, 2014; Lanje *et al.*, 2010).

$$D = \frac{k\lambda}{\beta \cos\theta}$$

Where D is the particle size, k is a constant having a value of 0.97 and λ has a value of 1.5405Å. β is full width at half maximum (FWHM).

2.2.3 Fourier Transform Infrared Spectroscopy (FTIR)

FTIR is a method used to determine the structures of molecules utilizing their characteristic absorption of infrared radiation. The nanostructures selectively absorb radiation which results in changes in their dipole moment. Subsequently, energy levels

transfer to excited state. The frequency number and intensity of the absorbance peaks are linked with the vibrational energy gap, vibrational freedom, and changes in the dipole moment of the samples' molecules. Thus by analyzing an infrared spectrum, ample amounts of information of the samples being studied can be obtained.

The range of Infrared region is 12800 ~ 10 $cm^{-1}$and can be divided into near-infrared region (12800 ~ 4000 cm^{-1}), mid-infrared region (4000 ~ 200 cm^{-1}) and far-infrared region (50 ~ 1000 cm^{-1}). The common used region for infrared absorption spectroscopy is 4000 ~ 400 cm^{-1} (How an FTIR Spectrometer Operates, 2013).

Samples were prepared for FTIR, for which potassium bromide (KBr) (Sigma-Aldrich, USA) was used. The samples, 0.2mg were each ground with 400mg of KBr and pressed with a hydraulic presser (Shanghai Regulator Factory Co., Ltd.) to form pellets for infrared spectroscopy.

2.3 *In Vitro* Experiments

The experiments were performed on *in vitro* cell cultures, cancer cell line Human Hepatocellular Carcinoma HepG2 (ATCC® HB-8065™) was grown under controlled experimental conditions in the lab in sterile environment using Laminar Flow Hood (BSB48, ICN Flow).

2.3.1 Cell Culture Conditions

HepG2 were maintained as monolayer cultures in 25cm^2 and 75cm^2 culture flasks (Corning® Flasks, Corning Incorporated Corning, NY14831 USA) in Roswell Park Memorial Institute (RPMI) 1640 (Sigma-Aldrich, USA), and Dulbecco's Modified Eagle's Medium (DMEM) (Sigma-Aldrich, USA) supplemented with 10% FCS (GibcoBRL, Gaithersburg MD) and 1% GPPS (2mM L-Glutamine (Sigma-Aldrich, USA), 1mM Na-Pyruvate (Sigma-Aldrich, USA), 100U/ml Penicillin (Sigma-Aldrich, USA), 100µg/ml Streptomycin (Sigma-Aldrich, USA)) in a humidified 5% CO_2 incubator (Model CO27, New Brunswick Scientific).

2.3.3 Cell Thawing

Cryopreserved cell line was partially thawed and culture media was added drop wise in the cryovial (Corning Incorporated, Canada). The cell suspension was then transferred to a 15ml tube and centrifuged (IEC H-SII Centrifuge, International Equipment Company) at 1200rpm for 5 minutes. The cell pellet was dislodged and re-suspended in 10ml of culture medium and seeded in $75cm^2$ culture flask. The flask was placed in a horizontal position in the incubator and the cells were allowed to attach and grow at the respective culture conditions. Next day 5ml of the old media was removed and fresh media was added, the cells were allowed to grow for a week before using them in experiments.

2.3.4 Cell Passaging

Cultures were observed under inverted microscope (Olympus CK2) and 70-90% confluent cultures were passaged at a ratio of 1:8 once every week, by trypsinization with 1ml of 0.5mM trypsin/EDTA (Sigma-Aldrich, USA) for 1 minute at room temperature. The cells as observed under the microscope, became round and began floating, this showed the adherent cells had detached from the surface of the culture flask, culture medium was added to the culture flasks to inactivate the protease. The medium containing the cells was transferred to a 15ml tube and was centrifuged for 5 minutes at 1200 rpm. The supernatant was discarded and the pellet containing the cells was processed as required.

2.3.5 Cell Counting

Cells were counted by the Trypan Blue exclusion assay. Trypan blue is a diazo dye used to stain selectively dead cells in a sample. Number of viable or dead cells present in a cell suspension is determined by Trypan blue exclusion assay. The chromophore being negatively charged interacts with the damaged membrane only while live cells having intact membranes exclude the dye, therefore the name trypan blue exclusion assay. Dead cells have blue cytoplasm while viable cells have clear cytoplasm (Koester *et al.*, 1998; Strober, 2001; Atale *et al.*, 2014). This method cannot identify and distinguish between apoptotic and necrotic cells.

Culture medium containing the cells were mixed with equal amount of Trypan Blue (0.4%), and gently added onto a haemocytometer slide (Weber Scientific International Ltd, England) (Figure 2.4A) through a cover slip (VWR® Scientific) to avoid any bubble formation. Haemocytometer has a central chamber engraved with a grid having an area of $1mm^2$. The cells present in the central grid (Figure 2.4B) of the haemocytometer were counted; cells touching the upper and left border were counted while the cells touching the right and lower borders of the central grid were not counted, under the inverted compound microscope (Mascotti *et al.*, 2002). The cell concentration was calculated by the formula:

$$\text{Cell Count} = \text{Number of Live cells} \times \text{Dilution factor} \times 10^4$$

Where dilution factor is 2, and 10^4 represents volume of the counting chamber.

The harvested cells were either used for plating to be utilized further in an experiment or were re-seeded in the culture flasks.

2.3.6 Cell Freezing

Cells were harvested by trypsinization and pelleted, the pellet was then re-suspended in pre-chilled freeze mix (45% RPMI 1640 + 10% filtered DMSO + 45% FCS) to yield $5x10^5$ cells/ml. 1ml aliquots of the cell suspension were taken in cryovials and transferred to -70°C freezer immediately for at least 4 hours and were later transferred to liquid nitrogen for long term storage.

TM 17335

A)

B)

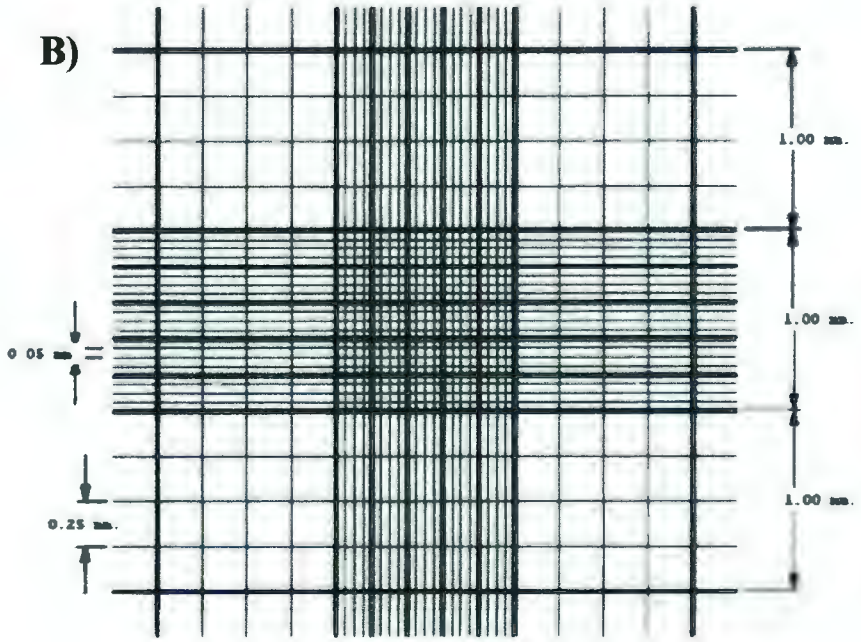

Figure 2.4 A) Haemocytometer slide B) Central grid of a haemocytometer. (Source: Automatic Cell Counter for Microscope).

2.4 Anticancer Activity of Doped and Undoped CuO

2.4.1 Cytotoxicity Screening

Initial cytotoxicity screening of the nanostructures was done against HepG2 cell line by Sulforhodamine B assay (Figure 2.5). Solutions of nanostructures (stock concentration: 10mg/ml) were prepared in deionized water and were sonicated (3210 Branson) for 30 minutes prior to screening. Pre-seeded HepG2 cells (10,000 cells/well) were treated with final concentration of 100µg/ml in a 96 well plate (Corning® Flasks, Corning Incorporated Corning, NY14831 USA), along with controls including untreated cells (NTC), Cisplatin (Cis) (United Pharm, Korea), and Doxorubicin (Dox) (United Pharm, Korea). The cells were fixed with 25µl/well of 50% Trichloroacetic Acid (TCA) (Merck Millipore Corporation, Germany) at 4°C for minimum 1 hour. Plate was washed with deionized water 3-4 times and air dried. Fixed cells were stained with 50µl/well of 0.01% Sulforhodamine B (SRB) (Sigma-Aldrich, USA) dye for 30 minutes, washed 3-4 times with 1% Acetic Acid to remove the unbound dye and air dried. The plate was photographed under light microscope, cells were counted and percentage viability was calculated.

2.4.2 IC_{50} Calculation

The inhibitory concentration which inhibits 50% of cellular growth i.e. IC_{50} values of nanostructures were calculated against HepG2 cell line by MTT assay. Mitochondrial function was assessed by MTT assay (Maqsood *et al.*, 2013). MTT 3-(4, 5-dimethylthiazol-2-yl)-2, 5-diphenyltetrazolium bromide is a tetrazolium dye, yellow in color that is reduced by metabolically active cells, by the action of dehydrogenase enzymes, to its insoluble product formazan (Figure 2.6), which is purple in color. Thus this assay is used to measure mitochondrial activity and cell proliferation induced by chemicals and drugs.

In a 96 well plate, pre-seeded cells ($1x10^4$ cells/well) were exposed to different concentrations of the nanostructures (100, 50, 10, 5 and 1µg/ml). After 24 hours of exposure 10µl of MTT dye (5mg/ml 1X PBS) (PhytoChemical) was added to each well

and samples were further incubated for 3 hours and 30 minutes. Afterwards, acidified 10% SDS (Sigma-Aldrich, USA) was added and plates were incubated at 37°C for overnight. Plates were analyzed and absorbance values recorded at 570nm wavelength with Microplate reader (Platos R 496, AMP). Controls; untreated cells, media only and nanostructures only were included in the assay.

Percentage viability relative to untreated sample (NTC) was calculated using the formula:

Relative Percentage Viability =

$$\frac{\text{Absorbance of sample} - \text{Absorbance of respective control}}{\text{Absorbance of untreated sample} - \text{Absorbance of media}} \times 100$$

IC_{50} values were calculated using the formula:

$$IC_{50} = b - \frac{[(b-a)\times(50\%-d)]}{(c-d)}$$

Where 'a' and 'b' represent the nanostructures' concentrations resulting in just more than 50% and just less than 50% viable cells respectively. 'c' is the percentage viability produced by 'a', and 'd' is the percentage viability produced by the concentration 'b'.

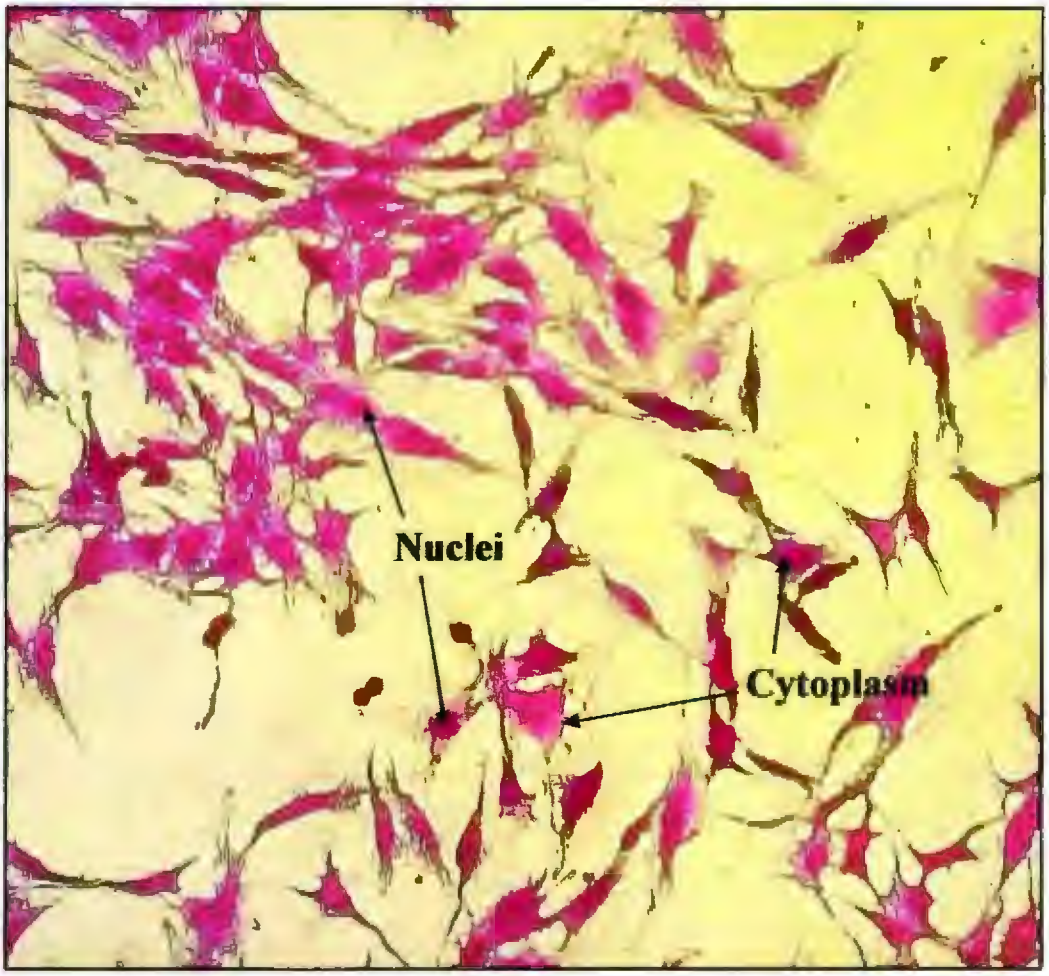

Figure 2.5 Hepatocellular carcinoma (HepG2) cells stained with 0.01% Sulforhodamine B (SRB) stain. Nuclei stained dark pink in the center of cells and cytoplasm light pink stained by the dye can be seen as indicated by the arrows.

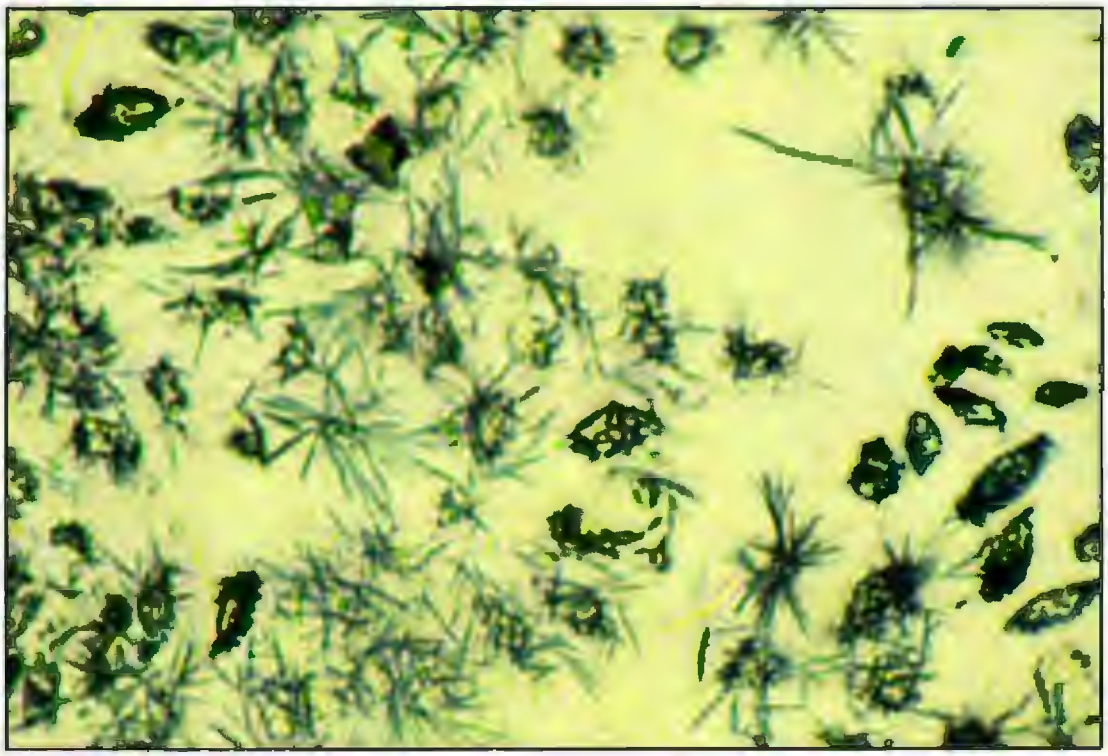

Figure 2.6 Formation of Formazan crystals after 3 hours incubation of cells with MTT. Viable cells with mitochondrial function reduce MTT to insoluble formazan crystals visible under microscope.

2.5 Investigating Immediate Effects of Nanostructures

Trypan Blue Exclusion Assay was performed to check the viability of HepG2 cells at respective time points after exposure with nanostructures. The assay worked on the principle as have been described previously (Section 2.3.4). Pre-seeded cells (10,000 cells/well) in a 24 well plate (Corning® Flasks, Corning Incorporated Corning, NY14831 USA) were treated with IC_{50} concentrations of the Nanoparticles. Doxorubicin, Cisplatin and untreated sample were included as positive and negative controls respectively. Cultures were exposed to the nanostructures for 10 minutes and 1 hour. The time points were chosen to verify cell death as apoptosis or necrosis.

At the completion of treatment time culture media was removed and 300µl of 1:1 Trypan Blue dye (GibcoBRL, Gaithersburg MD) prepared in 1X PBS was added into the respective wells. After 30 seconds, the dye was removed and 100µl of 1X PBS was added. The wells were photographed and analyzed.

2.6 Induction of Lipid Peroxidation

Lipid peroxidation i.e. oxidative degradation of the plasma membrane induced by the Ag-doped and un-doped CuO and Ag nanostructures, can be quantified by the extent of Thiobarbituric Acid Reactive Substances (TBARS) i.e. Malondialdehydes (MDA) produced. TBARS assay quantifies MDA that are byproducts of lipid peroxidation, enumerated colorimetrically following its reaction with Thiobarbituric Acid. The assay as described by (Arooj *et al.*, 2015) was performed.

Pre-seeded cells (10,000 cells/well) were exposed to 10µg of each nanostructure for 24 hours in triplicates in a 24 well plate. Untreated sample, Doxorubicin and Cisplatin treated cells were also included in the assay. Cells were harvested by trypsinization (Section 2.3.3) and collected in 1.5ml reaction tubes. Samples were centrifuged at 2000rpm for 5 minutes. Supernatant was discarded and the pellets kept on ice, meanwhile 150 µl cell lysis buffer was added in each well and the samples were incubated for at least 10 minutes

at 4°C and at -70°C for 10 minutes. The lysates were collected in the respective reaction tube and incubated at 4°C for 15 minutes and at -70°C for 15 minutes.

To the sample lysate equal volume of 10% SDS was added and incubated for 5 minutes at room temperature. Next, 2.5 times volume of lysate, Thiobarbituric Acid (TBA) (4.5mg/ml) (Sigma-Aldrich, USA) was added in each sample and incubated at 95°C in a water bath (Clifton) for 45 minutes, the samples were then instantly cooled by placing them on ice. They were then centrifuged at 14000rpm for 2 minutes to settle down the cellular debris. Absorbance readings were taken at 532nm by Nanodrop Spectrophotometer (Thermo Fisher Scientific). Non-cellular control (sample containing cell lysis buffer instead of lysate) was also included in the assay. Percent TBARS were calculated relative to untreated sample.

2.7 Detection of Apoptosis

2.7.1 Acridine Orange – Propidium Iodide (AO-PI) Staining

Acridine Orange (AO) stain being membrane permeable, binds with nuclei of viable cells and fluoresce green when visualized under blue fluorescent light. When AO enters acidic environment (apoptotic cells) it fluoresces orange under the same light. Propidium Iodide (PI) is impermeable in viable cells, and thus stains dead cells red under green fluorescent light. Overlapping of green and red images shows yellow and orange cells which depicts early and late apoptosis respectively (Foglieni *et al.*, 2001).

Pre-seeded cells (100,000 cells/well) in 6 well plates (Corning® Flasks, Corning Incorporated Corning, NY14831 USA) were treated with the IC_{50} concentrations of nanoparticles calculated through SRB assay for 3 hours. Cisplatin and untreated sample were also included as controls. Treated and untreated cells were stained with 100µg AO (Sigma-Aldrich, USA) and 100µg of PI (Sigma-Aldrich, USA). Media from the wells was removed and 300µl of AO-PI mixture (1:1) was added. The cells were visualized under fluorescent microscope in blue and green light. Photographs were taken and analyzed.

2.7.2 DNA Ladder Assay

DNA ladder assay is a qualitative assay used to detect apoptosis. Apoptotic DNA fragmentation is a significant characteristic of apoptosis, DNA fragments of 180bp and multiples thereof can be visualized through gel electrophoresis.

DNA ladder assay was performed to determine DNA fragmentation in HepG2 cells after treatment with nanostructures at their IC_{50} values. Doxorubicin, Cisplatin, and untreated cells were also included as positive and negative controls respectively. Cells ($4x10^4$/well) were seeded into 6-well plates. The cells were exposed to respective treatment for 24 hours and incubated at 37°C in humidified CO_2 incubator. The cells were trypsinized and harvested, the pellets washed with 1X PBS (pH: 7.4) twice. DNA extraction from the cells was done by Salting out method.

2.7.2.1 DNA Extraction:

Pellet containing cells was dislodged and 500µl of cell lysis buffer (LB2) was added to prepare the lysate. Samples were incubated at 4°C for at least 10 minutes and at -70°C for at least 10 minutes. The volume was maintained by adding 4.5ml T.E. Buffer. Proteinase K (Thermo Fisher Scientific, USA) (12.5µl) and 10% SDS (250µl) were added and the samples were incubated for overnight at 37°C (Orbit Shaker Bath, Labline, USA).

On day two, proteins were precipitated out by adding 1ml of 5M NaCl to the samples followed by vigorous shaking for 30 seconds. The samples were placed on ice for 10 minutes and then centrifuged at 1500 rpm for 10 minutes at 4°C. The supernatant was collected in separate set of properly labeled tubes, and centrifuged again. Equal volume (i.e. 5.5ml) of isopropanol (RDH Corporation, Germany) and 500µl of 10M Ammonium Acetate (Sigma-Aldrich, USA) were added to the samples for DNA precipitation. Thread like structures could be seen in the reaction tubes. To achieve maximum DNA precipitation the samples were incubated for overnight at -20°C.

The samples were centrifuged at 3200rpm for 60 minutes at 4°C, supernatants were discarded and DNA pellets were washed with 70% ethanol, followed by centrifugation at

3200 rpm for 30 minutes at 4°C. The DNA pellets were air dried and re-suspended in 50µl T.E. Buffer. Concentration of DNA was evaluated using Nanodrop spectrophotometer.

2.7.2.2 Agarose Gel Preparation:

Agarose gel was used for electrophoresis. 2% agarose gel was prepared. 2g of agarose was weighed for 100ml 1X TBE buffer. The mixture was heated in a microwave and the bottle was shaken occasionally, until the gel dissolved completely and the solution became transparent.

The hot solution was kept in a water bath at 55°C for approximately 30 minutes to cool it down. The gel was then poured in the gel tray in which the combs had been set and the sides were sealed with paper tape. The gel was allowed to solidify for approximately 15-20 minutes. Afterwards the combs were carefully removed and the gel was stored in 1X TBE buffer until it was required for use.

2.7.2.3 Gel Electrophoresis:

Genomic DNA 4µg along with Orange G (loading dye) (Merck Millipore Corporation, Germany) was loaded on 2% agarose gel (Hydra Gene Co., Ltd) containing 7µl Ethidium Bromide (50µg/ml) (Sigma-Aldrich, USA) and electrophoresed for 1 hour at 110V (BioRad Power Pac 3000, HC, USA). DNA from treated and untreated cells along with GeneRuler 100bp DNA ladder (Thermo Fisher Scientific, USA) was also loaded alongside as size marker. DNA was visualized under UV trans-illuminator (UVITEC Cambridge, UVI SAVE HD2) and the results documented with gel documentation system.

The composition of solutions used in various methods is given in Table 2.2.

2.8 Statistical Analysis

Data obtained from various experiments was statistically analyzed using Microsoft Excel 2013. The data was represented as mean ± SD. Statistically significant differences were calculated using t-test (two tail). A value of $p \leq 0.05$ was considered significant.

Table 2.2: Composition of Solutions

Solutions	Composition
Agarose (2%)	For 120ml: 2.4g agarose 120ml TBE buffer. Melt and dissolve in microwave. Shake at regular intervals. Cool down to 55°C.
Cell Lysis Buffer	For 500ml: 75ml of 150mM NaCl 10ml of 20mM Tris 0.50ml of 1mM Dithiothreitol (DTT) 0.5ml of 1% Triton X-100 Mix, make up volume to 500ml and store at 4°C.
Freeze Media	45% feed media 10% filter sterilized DMSO 45% FCS
Ladder (100 bp)	For 500µl: 100µl of 100 bp ladder (Thermo Fischer Scientific, USA) 100µl loading dye 300µl deionized water
MTT	For 10ml 50mg MTT 10ml 1XPBS (Store at 4°C)
NaCl (5M)	For 1 liter: 292.28g NaCl Make up volume to 1 liter
Phosphate buffer Saline (PBS) (10X)	137mM NaCl

	2.7mM KCl 8mM Na_2HPO_4 2mM KH_2PO_4 (pH 7.4) Mix and store at room temperature.
Phosphate buffer Saline (PBS) (1X)	For 500ml: 50ml 10X PBS 450ml deionized water
RPMI 1640	RPMI (filter sterilized) 10% FCS 1% GPPS
SDS (10%)	For 100ml: 10g SDS 80ml deionized water Mix on stirrer at low speed. Make up volume to 100ml
Sulforhodamine B (SRB) stain (0.01%)	For 100ml: 10mg SRB dye 100ml of 1% acetic acid Store at room temperature.
TCA (50%)	For 25ml: 12.5g TCA 25ml deionized water Mix and store at 4°C
Tris – Borate – EDTA (TBE) Buffer (10X)	0.89M Tris 0.025M Boric Acid 0.5M EDTA (pH 8.0)
Tris – Borate – EDTA (TBE) Buffer (1X)	For 500ml: 50ml 10X TBE 450ml deionized water

RESULTS

RESULTS

This study was conducted to study the cytotoxic and genotoxic potential of copper oxide (CuO), silver (Ag), and Ag doped CuO nanostructures. Doped nanostructures included 1%, 3%, 5% and 8% of Ag. These doped and undoped nanostructures were prepared by chemical co-precipitation method.

3.1 Investigation of Nanostructures

The structure and chemical properties of nanostructures were probed with techniques including, SEM to study their morphology and particle size, XRD used for their structural analysis, and FTIR for the exploration of their elemental composition.

3.1.1 Morphological Examination

In order to know the size and shape of the prepared nanostructures, Scanning Electron Microscopy (SEM) was used with an electron beam of energy 15kV. It can be observed from the images that the prepared samples are nanostructures and the shape of the nanostructures changed when doped with Ag (Figure 3.1).

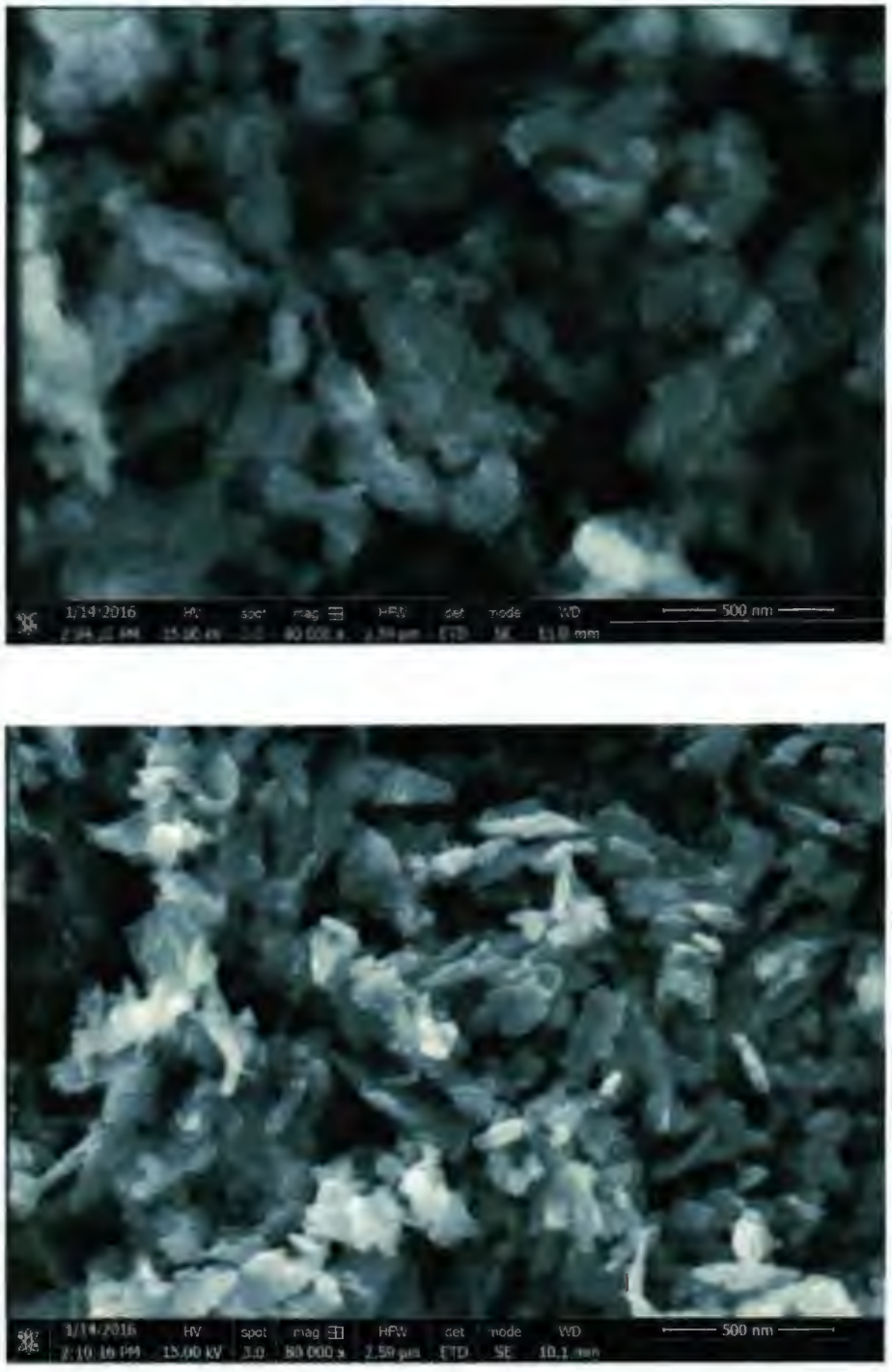

Figure 3.1 Scanning Electron Microscopy (SEM) images of synthesized nanostructures. (A) Undoped and (B) 8% doped CuO Nanostructures.

3.1.2 Structural Properties

X-Ray diffraction patterns were recorded at $2\theta = 30 - 60°$ to study the crystallinity of the undoped and Ag doped CuO nanostructures prepared by wet chemical route. The obtained XRD patterns are shown in Figure 3.2. It can be clearly observed that the diffraction peaks in patterns can be indexed to (110), (002), (200), ($\bar{2}$02), (020), and (202) planes corresponding to the monoclinic structure of CuO. It can also be observed in the figure that the diffraction peak intensities increase with the increase in Ag content illustrating the increase in crystallinity of the nanostructures. The figure depicts a slight shift in diffraction peak towards a lower angle (2θ).

A clear peak indexed to (200) plane of Ag can be seen which suggests that some Ag ions are not doped into CuO matrix, but segregated into grain boundaries and created their own crystal phase. This might be attributed to the larger ionic radii of Ag ions as compared to Cu ions.

The crystallite sizes have been calculated using Scherrer's formula for undoped and Ag doped CuO. The average crystallite sizes as calculated are in the range of 17 – 26 nm which os compatible to the morphological results.

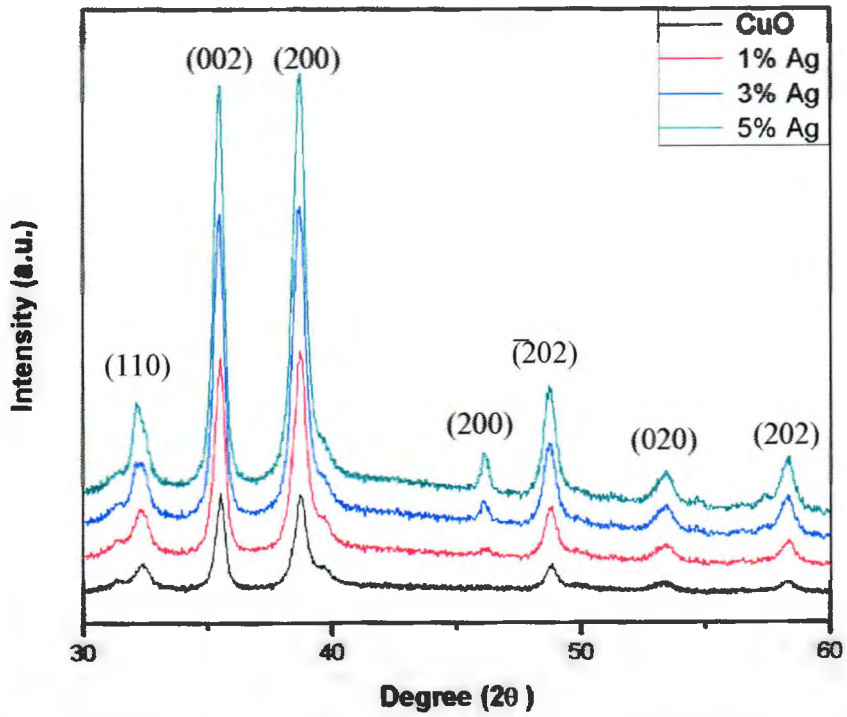

Figure 3.2 XRD patterns of CuO and Ag doped CuO (1%, 3%, and 5%).

3.1.2 Vibrational Modes Spectroscopy Characteristics

Fourier Transform Infrared Spectroscopy was used to obtain an infrared spectrum of absorption of undoped and Ag doped CuO nanostructures. The infrared spectra of nanostructures are shown in Figure 3.3.

FTIR spectra of pure CuO, and Ag doped CuO nanostructures demonstrates the number of vibrational modes in wave number range of 500 to 800 cm^{-1}. The vibrational modes at 400 – 800 cm^{-1} are related to Cu – O vibrations of the monoclinic structure of CuO. Absorption modes related to secondary phases of Cu_2O or AgO or other impurities were absent indicating the successful doping of Ag ions on CuO matrix.

The presence of all vibrational modes belonging to CuO monoclinic structure and absence of Ag dopant related vibrational modes indicates the successful doping of Ag into the CuO matrix.

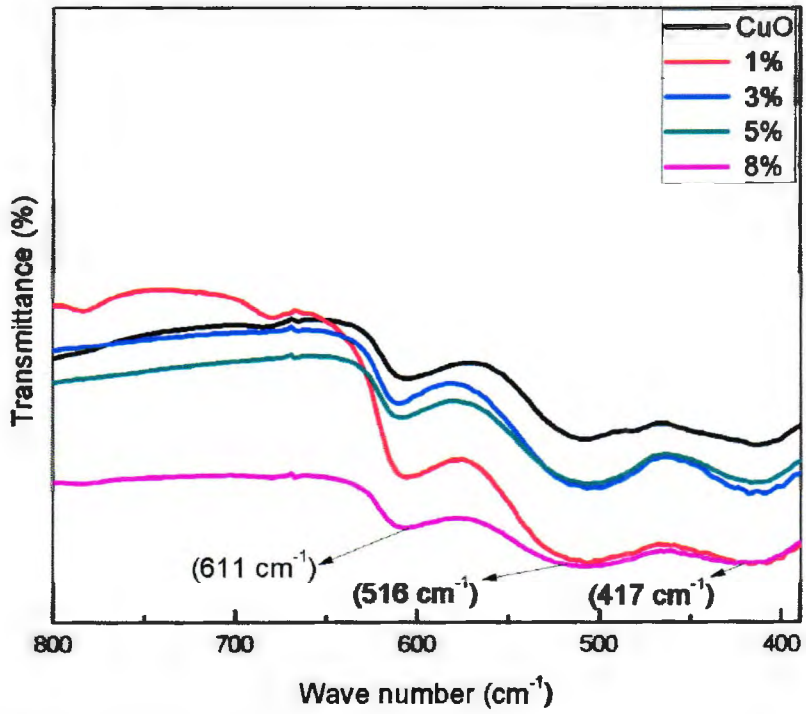

Figure 3.3 Fourier Transform Infrared Spectroscopy (FTIR) results of undoped CuO and doped CuO (1%, 3%, 5%, and 8%).

3.2 *In Vitro* Experiments

This study was conducted with aqueous suspensions of nanostructures. These nanostructures were exposed to hepatocellular carcinoma (HepG2) cell line. Their ability to cause cytotoxicity, their dose dependent response, and their ability to cause oxidative stress, genotoxicity i.e. DNA damage, and cell death mechanism via apoptosis or necrosis were investigated.

3.2.1 Cytotoxicity Screening

In order to test the cytotoxic potential of the nanostructures, HepG2 cells were treated with 100µg/ml of nanostructures for 24 hours. Untreated sample (NTC) was used as a negative control, and Doxorubicin (Dox) and Cisplatin (Cis) were included as positive controls.

SRB staining results revealed loss in viability and morphological changes in cells treated with nanostructures (Figure 3.4). Cells became small and round, cytoplasm shrinkage was also observed. Cells treated with Cisplatin showed 30% viability along with morphological changes. Doxorubicin had 20% decrease in viability and no change in morphology of cells was observed.

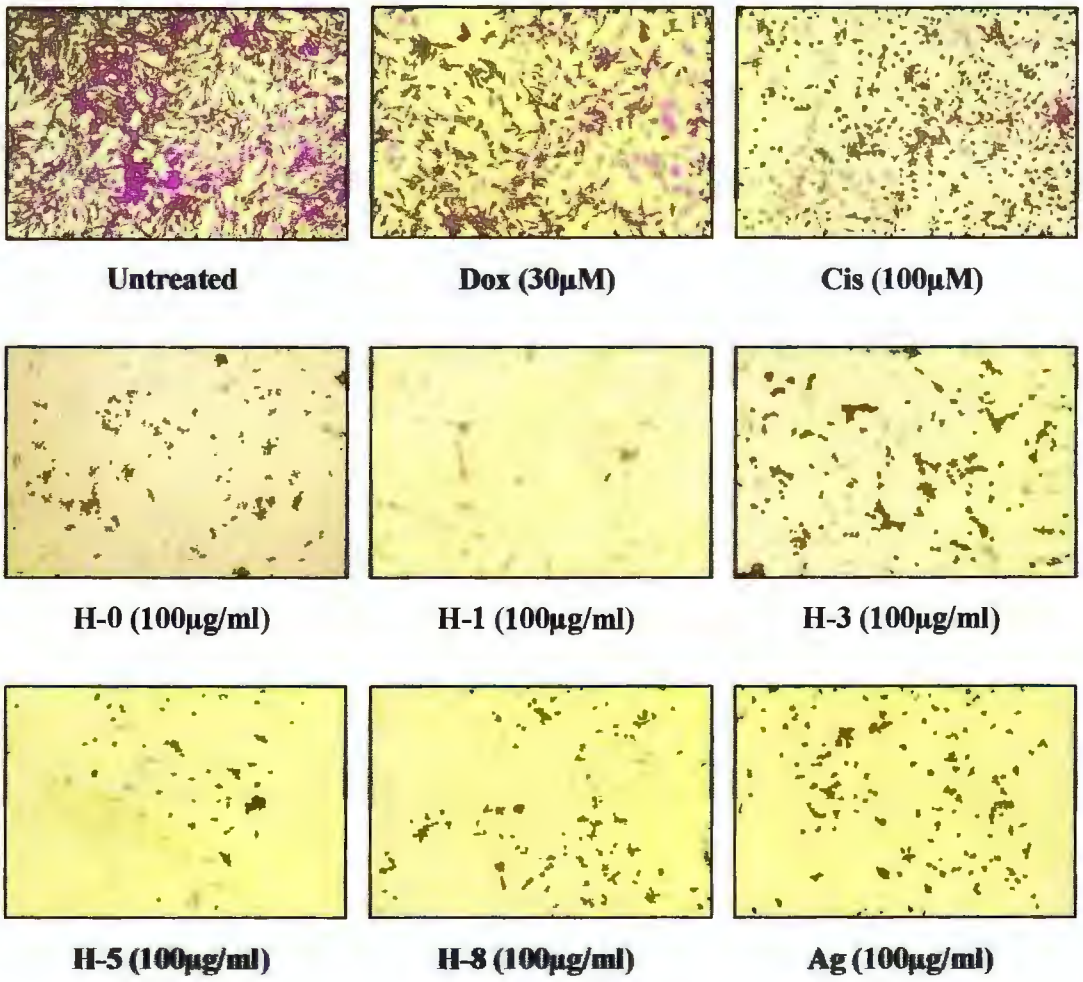

Figure 3.4 Cytotoxicity Screening of Nanostructures. HepG2 cells were treated with H-0, H-1, H-3, H-5, H-8 and Ag at 100μg/ml concentration. Untreated cells, Doxorubicin (Dox) and Cisplatin (Cis) were used as controls in the assay.

3.2.2 IC_{50} concentrations

HepG2 cells were treated with different concentrations (100, 50, 10, 5, and 1μg/ml) of doped and undoped nanostructures for 24 hours. Percent viabilities calculated via SRB assay and MTT assay were determined relative to untreated cells (NTC) and dose dependent drug response curves were used to calculate the IC_{50} concentrations for these nanostructures.

All nanostructures induced 50% cell death at the tested concentrations (IC_{50} < 100μg/ml) and showed decrease in cell viability in a dose dependent manner. The treated samples had a significant increase in viability as the concentration of the nanostructures decreased, this comparison with their significance difference is shown in Figure 3.5. The difference between nanostructures at their equal concentrations is depicted in Figure 3.6.

Decrease in IC_{50} values was observed for the doped nanostructures (IC_{50}: 7.8 – 9.7μg/ml), as compared to CuO (IC_{50}:14.85μg/ml) and Ag (IC_{50}: 43.66μg/ml). IC_{50} concentrations of the nanostructures are given in Figure 3.7.

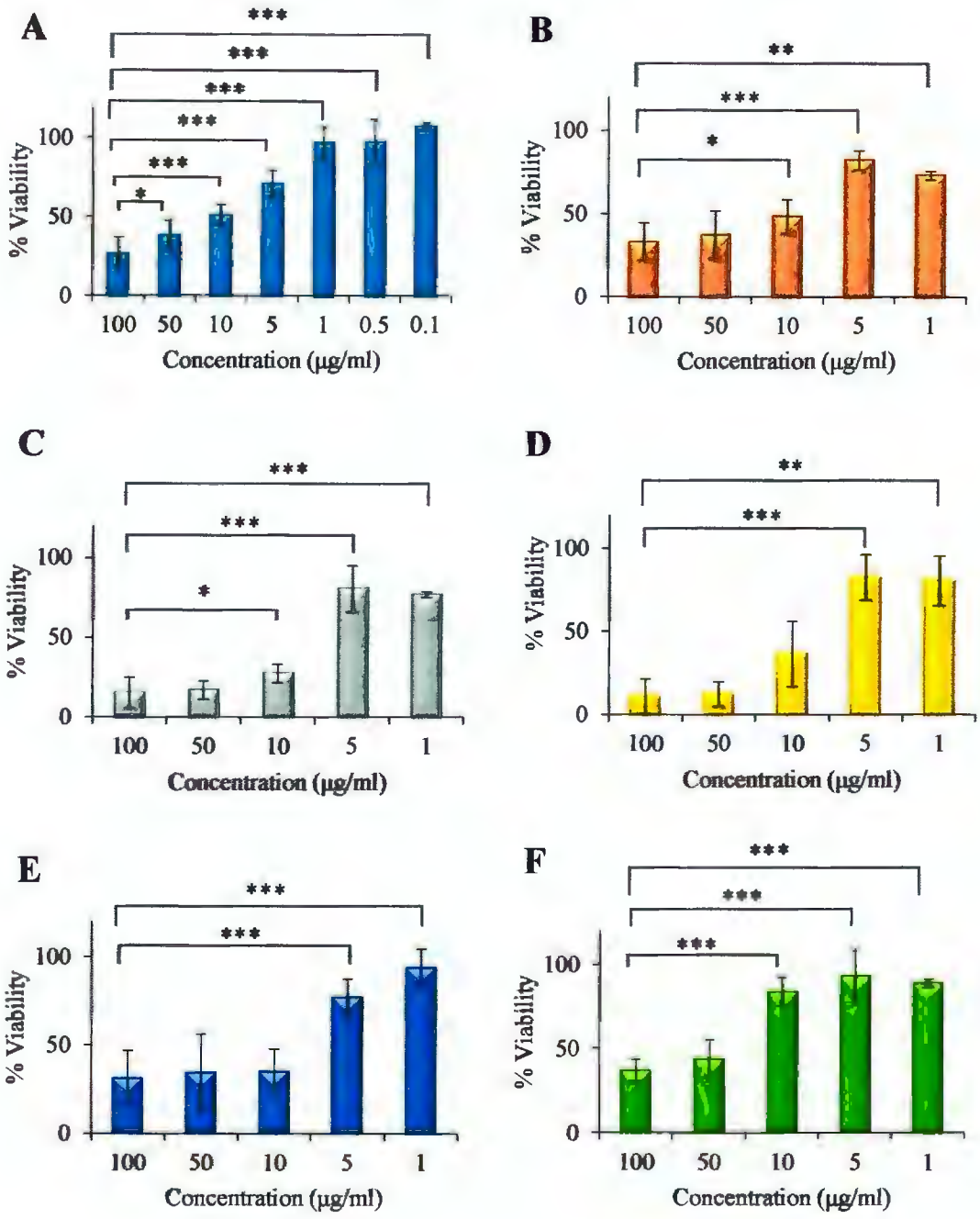

Figure 3.5 Cytotoxic Effects of Nanostructures. (A) H-0, (B) H-1, (C) H-3, (D) H-5, (E) H-8, and (F) Ag. Percentage Viabilities (mean ± SD) calculated relative to untreated sample. *$p \leq 0.05$ (two tail t-test) **$p \leq 0.005$ (two tail t-test) ***$p \leq 0.0005$ (two tail t-test).

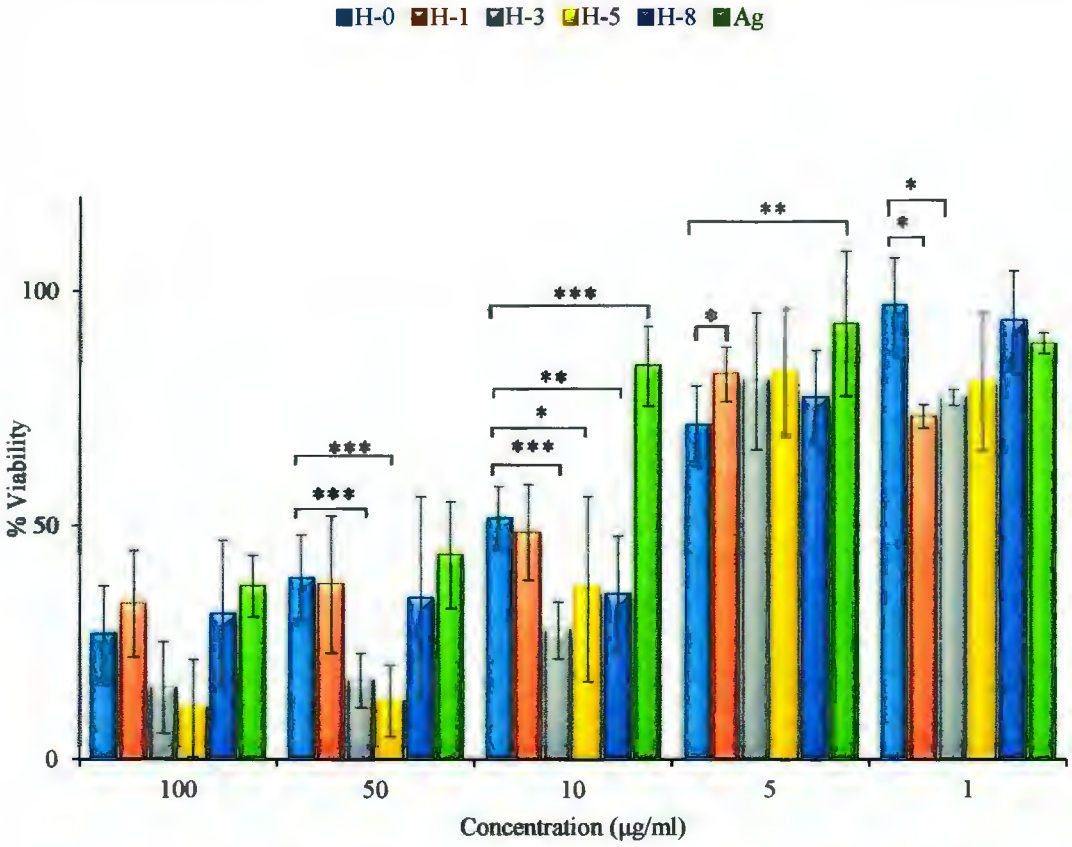

Figure 3.6 Comparative Analysis of Cytotoxicity Induced by Nanostructures. Percentage Viability (mean ± SD) relative to untreated sample. *$p \leq 0.05$ (two tail t-test) **$p \leq 0.005$ (two tail t-test) ***$p \leq 0.0005$ (two tail t-test).

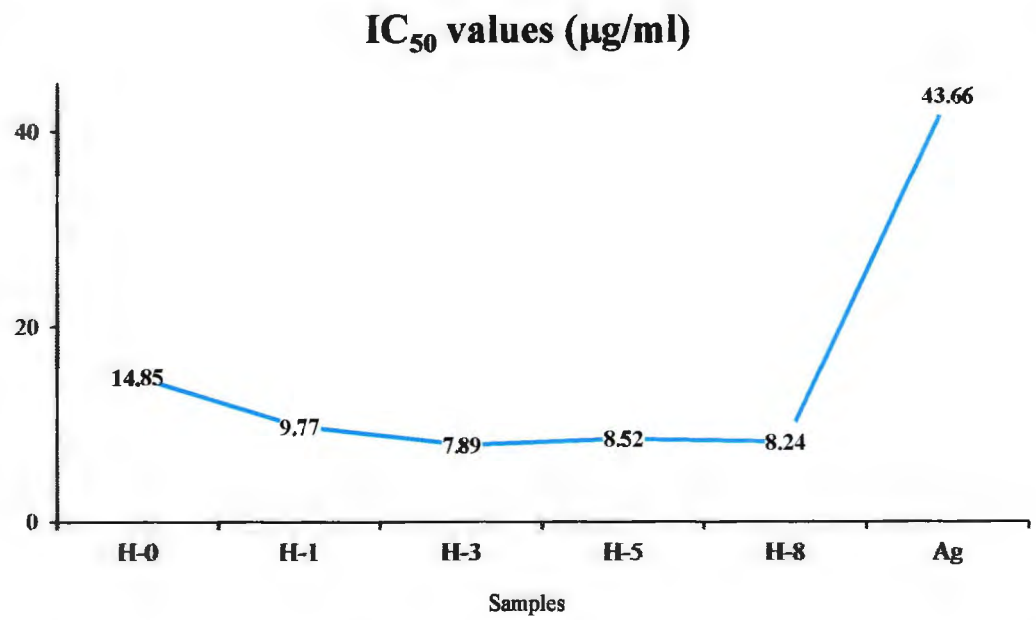

Figure 3.7 IC_{50} values of H-0, H-1, H-3, H-5, H-8 and Ag nanostructures against HepG2 cells. IC_{50} were calculated using percentage viabilities at various time points.

3.2.3 Investigating Immediate Effects of Nanostructures

The immediate effects of nanostructures was investigated using Trypan Blue Exclusion Assay. Pre-seeded HepG2 cells were treated with nanostructures at their IC_{50} values, followed by staining with Trypan Blue. Doxorubicin and Cisplatin at 100μM concentration were also included along with untreated sample as controls. The cells were visualized under light microscope after treatment for 10 minutes and 1 hour (Table 3.1) and counted.

Percentage viabilities for both time points were compared and significant difference ($p \leq 0.05$) between each sample was evaluated (Figure 3.8). Ag treated cells were least viable both time points i.e. 10 minutes and 1 hour of exposure and the difference in percentage viabilities at both time points in Ag treated cells was highly significant ($p \leq 0.0001$). H-1, H-3 and H-8 also showed significant difference in viability at both time points ($p \leq 0.005$). Doxorubicin and Cisplatin also induced significant difference in percentage viabilities at both time points ($p < 0.0001$).

Table 3.1: Results of Trypan Blue Exclusion Assay. Arrows show dead cells (blue).

Sample	Time Point: 10 min	Time Point: 1 hour
Un-treated		
H-0	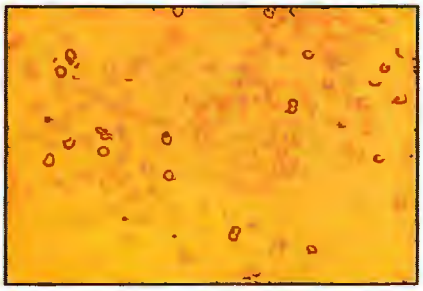	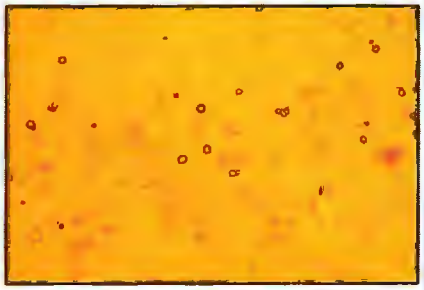
H-1	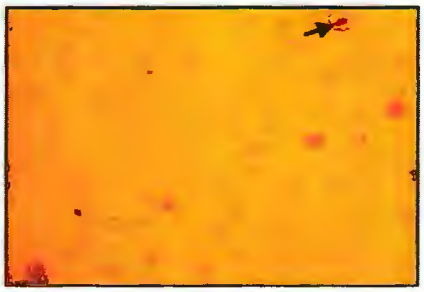	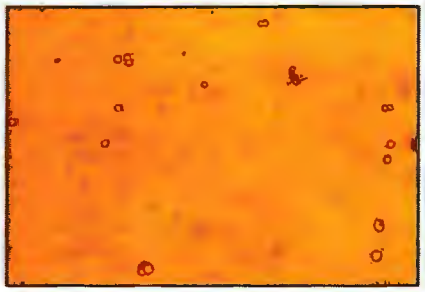
H-3	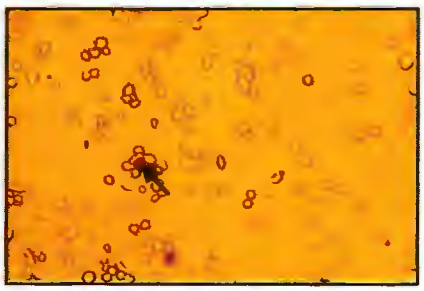	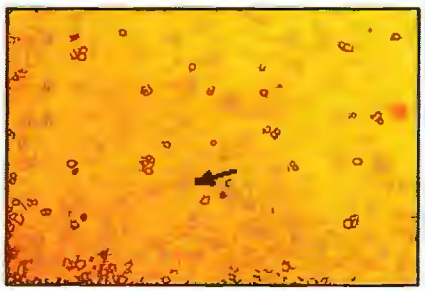

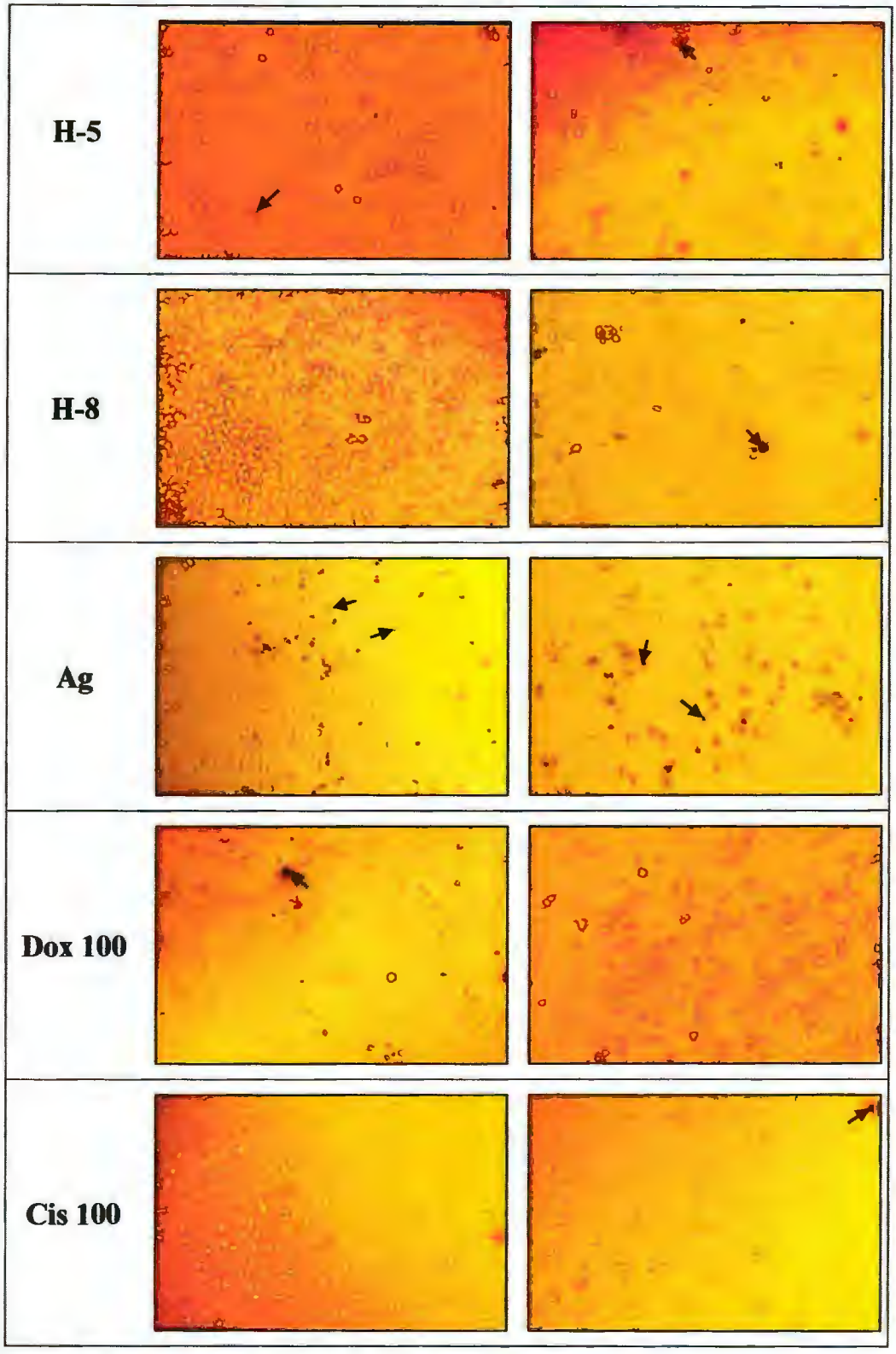
H-5
H-8
Ag
Dox 100
Cis 100

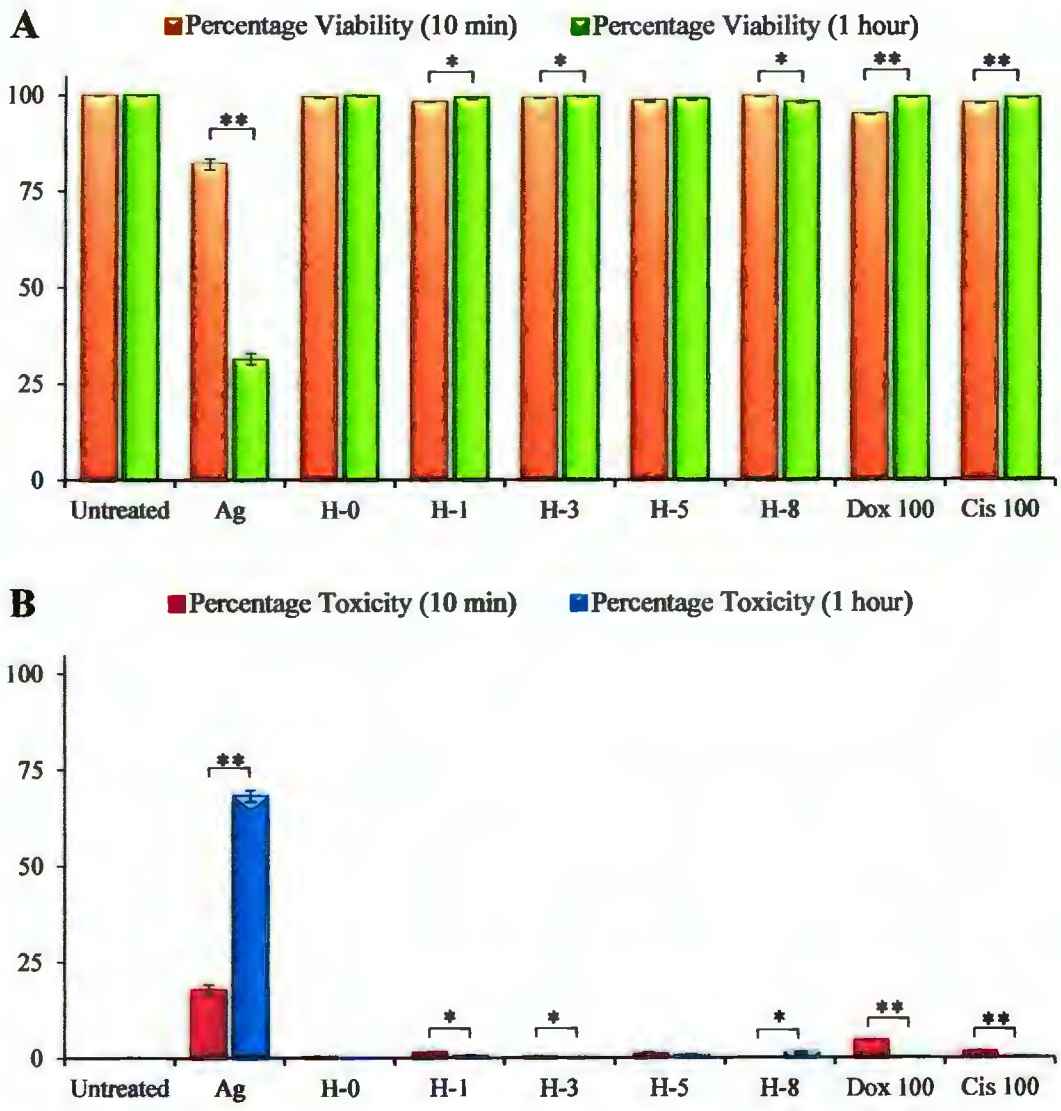

Figure 3.8 Comparison in (A) Percentage Viabilities, and (B) Percentage Toxicities at different time points. Percentage Viability and Toxicity (mean ± SD) sample at time points 10 minutes and 1 hour of exposure were calculated using Trypan Blue Exclusion Assay. *$p \leq 0.005$ (two tail t-test) **$p \leq 0.0001$ (two tail t-test).

3.2.4 Induction of Lipid Peroxidation

TBARS assay was performed to determine the extent of membrane lipid peroxidation caused by nanostructures on HepG2 cells. Cells were treated with 10μg/ml of nanostructures for 24 hours and lysed. Untreated sample, Doxorubicin (100μM), Cisplatin (100μM) and non-cellular control were also included in the assay.

MDA levels in all samples were calculated relative to untreated sample (Rel. MDA). Ag and Ag doped nanostructures; H-1, H-3, H-5, and H-8 showed highly significant increase in TBARS ($p \leq 0.01$). H-0 (Rel. MDA: 3.25) showed no significant lipid peroxidation, while Ag and Ag doped nanostructures; H-1, H-3, H-5 and H-8 induced significant ($p \leq 0.01$) lipid peroxidation in HepG2 cells (Rel. MDA: 3.30 – 5.23).

Cells treated with Cisplatin and Doxorubicin also produced significant levels of MDA ($p \leq 0.01$). The results are illustrated in Figure 3.9.

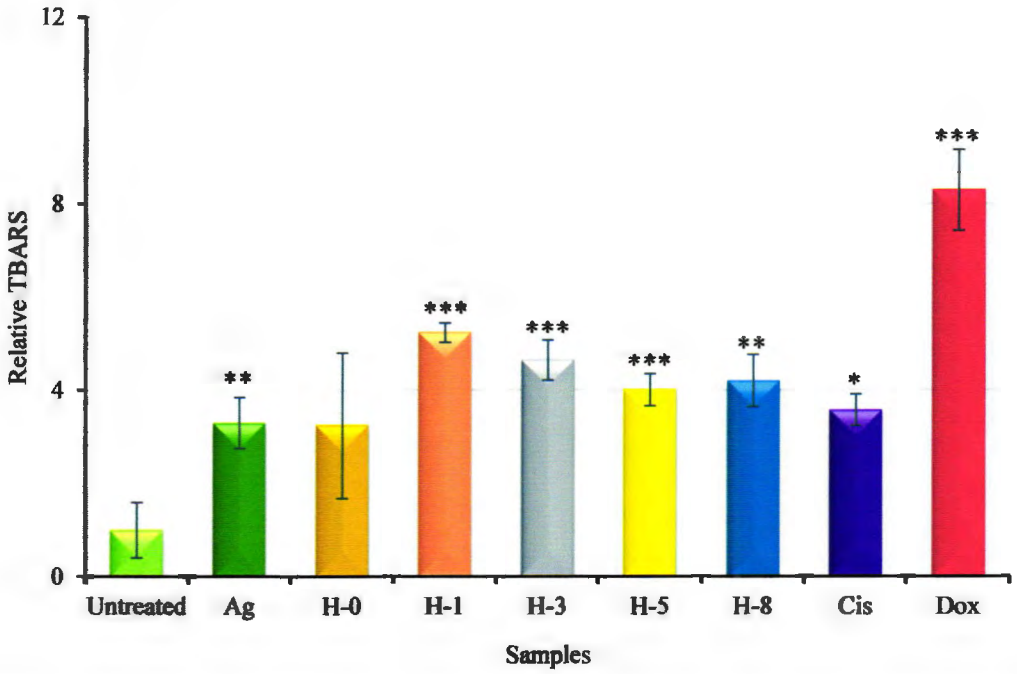

Figure 3.9 TBARS assay results for nanostructure treatment of HepG2 cells. Percent TBARS (mean ± SD) relative to untreated sample. *$p \leq 0.05$ (two tail t-test) **$p \leq 0.01$ (two tail t-test) ***$p \leq 0.005$ (two tail t-test) when compared to untreated sample.

3.2.5 AO – PI Staining

Pre-seeded HepG2 cells were treated with nanostructures at their IC_{50} values for 3 hours, followed by staining with a mixture of Acridine Orange (AO; 100µg/ml) – Propidium Iodide (PI; 100µg/ml), simultaneously. AO fluoresced green under blue light in viable cells, and orange in apoptotic cells; whereas PI stained the nuclei of necrotic cells red under green light. Untreated sample was used as a negative control while Cisplatin was used as a positive control.

When untreated sample and treated cells were observed under fluorescent microscope, in green and blue light. Green cells were visible under blue light while red cells were observed under green light. The cells observed were photographed in each light and pictures were overlapped (Table 3.2). In the overlapped pictures, viable cells appeared green, while cells were stained yellow and orange in case of early and late of apoptosis, and necrotic cells appeared red. Cells were counted and percentage viability and percentage apoptosis were calculated relative to untreated sample.

Cells treated with H-0, H-3 and Ag showed significant decrease in percentage viability and a significant decrease in percentage apoptosis as compared to untreated sample ($p \leq 0.05$). H-0, H-1, H-5, H-8, Cisplatin (Cis) did not have significant difference in viability or apoptosis. No significant percentage necrosis was seen in any treated cells (Figure 3.10).

Table 3.2: Results of Acridine Orange and Propidium Iodide (AO-PI) Staining

Sample	Blue Light	Green Light	Overlap
Un-treated	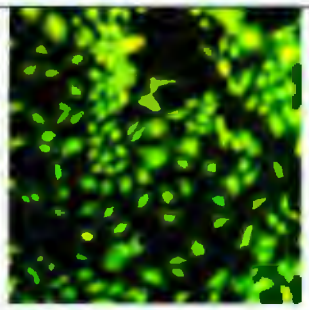		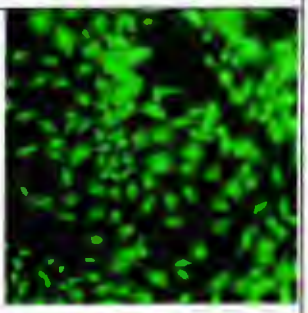
H-0	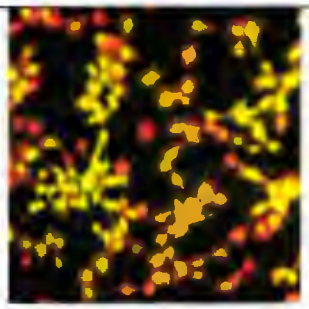	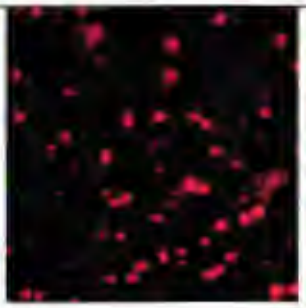	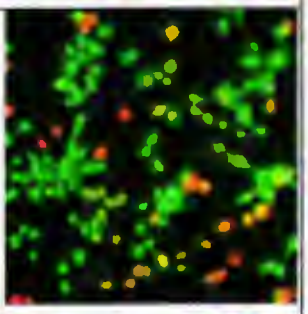
H-1	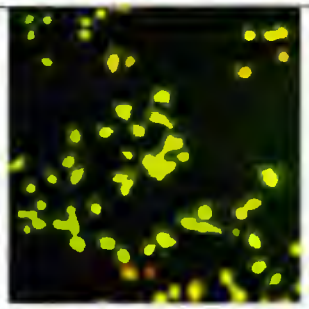		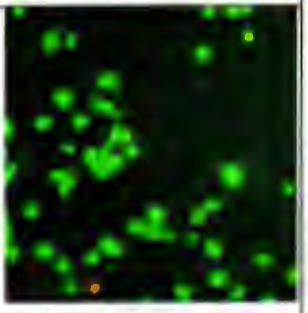
H-3			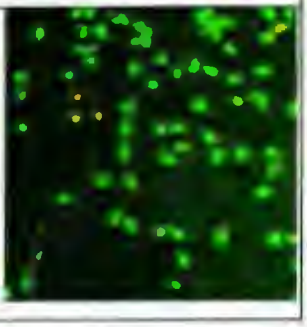

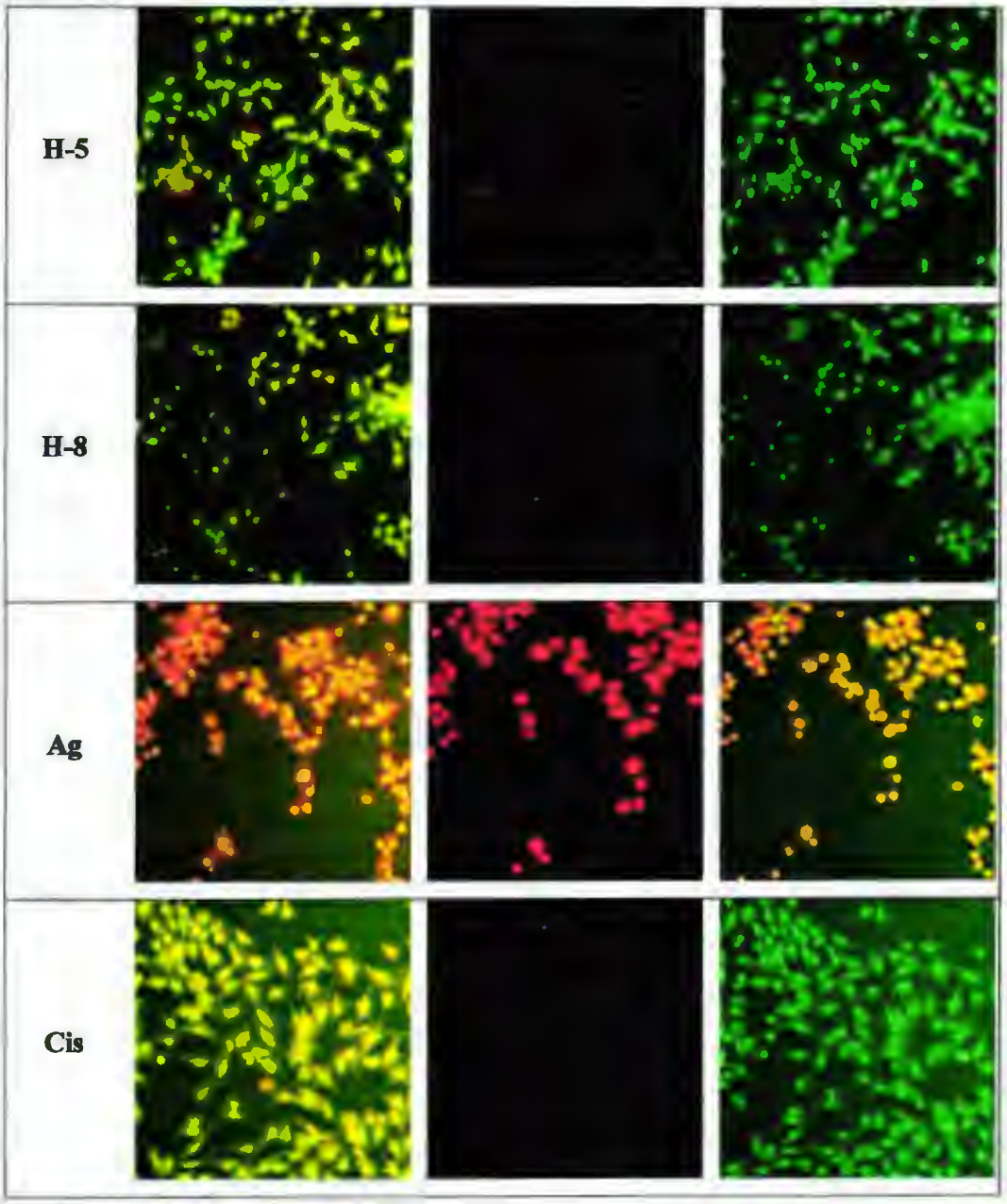
H-5
H-8
Ag
Cis

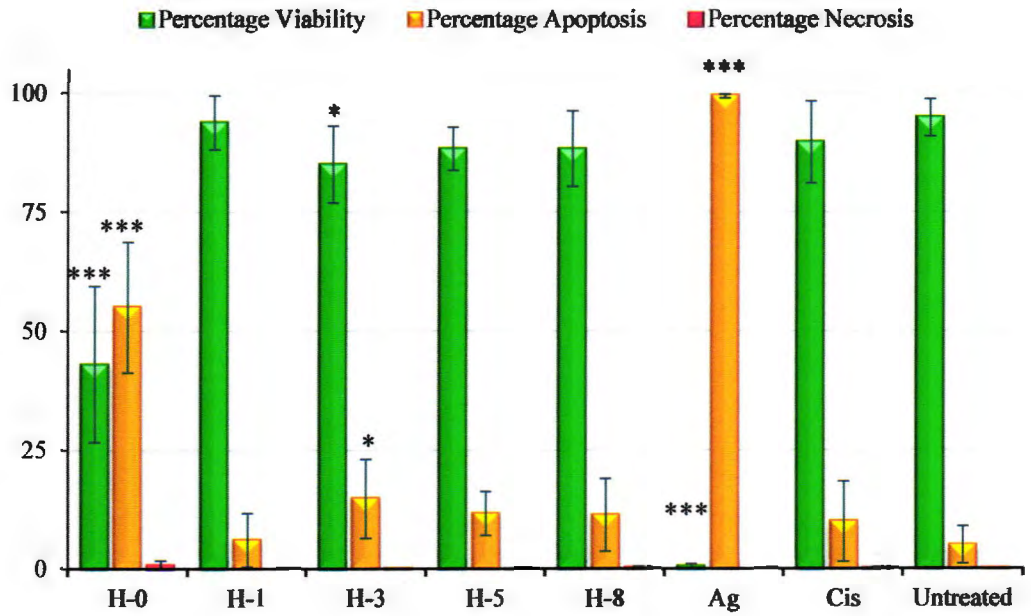

Figure 3.10 Percentage Viability Percentage Apoptosis and Percentage Necrosis. Percentage Viability, Apoptosis and Necrosis (mean ± SD) in treated cells was calculated using Acridine Orange and Propidium Iodide staining. *$p \leq 0.05$ (two tailed t-test) **$p \leq 0.005$ (two tail t-test) ***$p \leq 0.0005$ (two tail t-test) when compared to untreated sample.

3.2.6 DNA Ladder Assay

DNA Ladder Assay was performed to detect the apoptotic DNA fragmentation in treated cells. HepG2 cells were treated with 10μg/ml of nanostructures for 24 hours. Untreated cells and Dox (50μM) treated cells were also included as controls in the assay.

After 24 hours of exposure, as compared to untreated sample, H-0 showed approximately 30% reduction in the genomic band, while 80 – 90% reduction in intensity of bands was seen for H-1 and Ag. H-3, H-5, and H-8 showed 30-50% intensity reduction in bands. Dox (50μM) also had moderate effect and 30% band intensity was reduced relative to untreated sample. Figure 3.11 illustrates the ladder assay results.

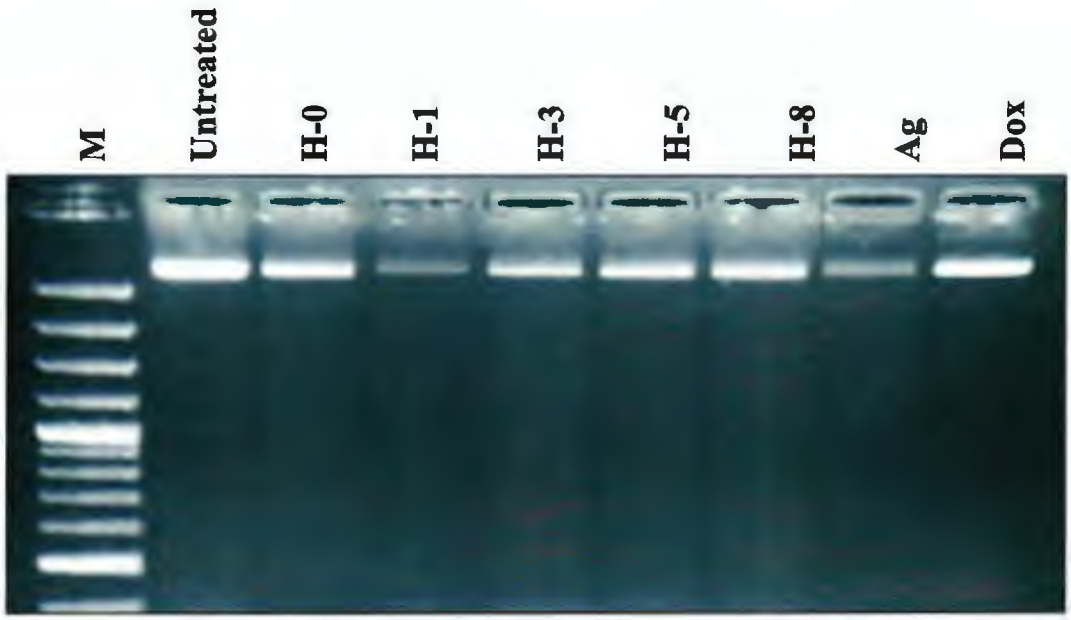

Figure 3.11 Detection of DNA degradation in HepG2 cells. Cells were treated with H-0, H-1, H-3, H-5, and H-8 and Ag nanostructures at 10μg/ml. Untreated cells and Doxorubicin (Dox; 50μM) were included as controls in the ladder assay alongwith 100bp DNA ladder used size reference marker (M).

DISCUSSION